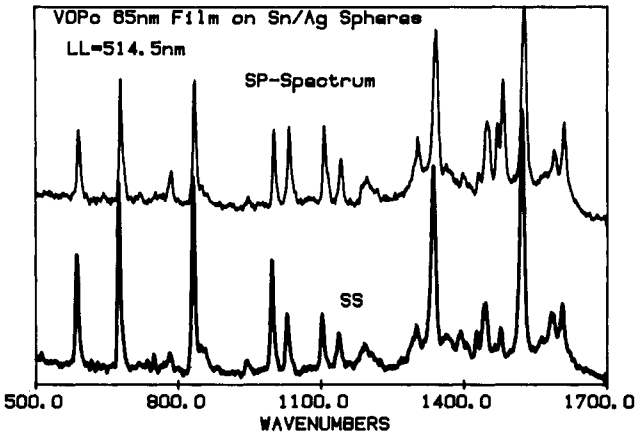

Figure 7. Spontaneous RS of a 65-nm VOPc film grown onto Ag-coated Sn spheres, illustrating the polarization properties of the film. Top: S polarization of the incident light and P polarization of collected light. Bottom: SS spectrum.

Ag coated Sn spheres recovered the spectroscopic properties observed from the film evaporated onto a KBr substrate given in Figure 3. Molecular frequencies of VOPc selected from SERS and infrared spectra and their approximate interpretation are given in Table I. Symmetry assignments were carried out assuming a C_{4v} molecular point group. In this case e and a_1 types only are infrared active. Therefore, a strong IR signal with a weak Raman counterpart in the SS spectrum is most likely an e vibration. The reverse trend in intensities was found to be common for the a_1 type. Bands that were observed exclusively in the Raman could be assigned to b_1 or b_2 representations.

Conclusion

The application of SERS for vibrational characterization of molecular solids was illustrated with the VOPc case. The vibrational spectra of isolated molecules were obtained by using SERS of physisorbed molecules on metal surfaces at monolayer or submonolayer coverage. Molecular spectra served as reference for the study of perturbations of vibrational energy levels due to intermolecular interactions that may be evident in the spectra of large aggregates. Correlation field splittings in the solid films were confirmed by appearance of singlets in the molecular (SERS) spectra. Sn spheres coated with Ag were found to be SERS active in a broad range of visible spectral frequencies that enclosed the range of activity of Ag and Au island film with plasmon resonances in the blue and red, respectively.

Acknowledgment. Financial assistance from NSERCC and the URIF program of the Ontario Government is gratefully acknowledged.

Channel Inclusion Complexation of Organometallics: Dipolar Alignment for Second Harmonic Generation†

Wilson Tam,* David F. Eaton,* Joseph C. Calabrese, Ian D. Williams, Ying Wang, and Albert G. Anderson

E. I. du Pont de Nemours and Company, Central Research and Development Department, Experimental Station, PO Box 80328, Wilmington, Delaware 19880-0328

Received September 30, 1988

Guest–host channel inclusion complexation has been found to be a general method of forming acentric crystals capable of second harmonic generation (SHG) from 1.06-μm laser light. Formation of 30 inclusion complexes between hosts thiourea or tris-*o*-thymotide (TOT) and various organometallic (28) and organic (2) guests is reported. None of the hosts or guests are capable of significant SHG themselves. Of this total studied, 19 (63%) were SHG active. Five of the SHG-active compounds (all examined by X-ray crystallography) crystallize in polar space groups. For thiourea complexation of organometallic guests, 11 of 16 (69%) inclusion complexes were active. For TOT–organometallic complexation, only 6 of 12 (50%) were active. This difference is ascribed to the strong tendency of dipoles to dimerize in an antiparallel (centrosymmetric) orientation. Tight control of channel dimensions is required to prevent this electrostatic interaction which leads to zero SHG. If channel dimensions can be controlled and maintained small relative to guest dimensions, then head-to-tail dipolar orientation becomes electrostatically preferred. The structures of thiourea inclusion complexes of (η^6-benzene)$Cr(CO)_3$ (**1**), (η^4-1,3-cyclohexadiene)$Fe(CO)_3$ (**2**), (η^4-trimethylenemethane)$Fe(CO)_3$ (**3**), and (η^5-cyclohexadienyl)$Mn(CO)_3$ (**4**) have been determined by X-ray diffraction studies. Complexes **1**, **3**, and **4** are isomorphous and crystallize in the space group *R*3*c* while **2** crystallizes in the space group $Pna2_1$. TOT·(η^6-tetralin)$Cr(CO)_3$ (**5**) crystallizes in the space group $Pca2_1$. In the structures of **1**, **3**, **4**, and **5**, the guests are aligned head-to-tail along the channel direction. Channel inclusion complexation cannot guarantee an acentric structure for cases where the channels are large enough to accommodate a head-to-tail antiparallel pair. This situation is observed for TOT·$W(CO)_5$(4-X-pyridine) (X = H, NH_2; space group *I*2/*a*). The head-to-tail dipolar alignment may also not result if other strong packing forces (e.g., hydrogen bonding and π–π interaction of aromatic rings) can favor alternative arrangements. Such interactions are postulated for **2** and for TOT·$W(CO)_5$(4-Y-pyridine) (Y = Me, Et).

Introduction

Second harmonic generation (SHG) is a nonlinear optical process that converts an input optical wave into an output wave of twice the input frequency. The process occurs within a nonlinear medium. Chemists are familiar with SHG through its widespread use in laser chemistry to frequency double, e.g., a Nd:YAG laser, operating at 1060 nm to the green region (530 nm). Recent activity in many laboratories has been directed toward understanding

† Contribution no. 4715.

0897-4756/89/2801-0128$01.50/0

and enhancing second- and third-order nonlinear effects in inorganic, organic, and polymeric materials. Major research efforts are directed toward (a) identifying new molecules possessing large nonlinear polarizabilities and (b) controlling molecular orientation on a microscopic level to influence bulk nonlinear optical properties. Several recent reviews attest to the high interest in this area.[1]

Effective second harmonic generation materials have both high second-order molecular hyperpolarizability, β, and high second-order bulk susceptability, $\chi^{(2)}$. Many organic materials are highly polarizable and are thus inherently good candidates for second harmonic generation. Oudar[2] has suggested that a simple two-level model is adequate for predictive use in search for new materials. Within this framework, polar materials that possess low-lying charge-transfer states, or that experience large changes in molecular dipole moment on photoexcitation are potential SHG-active materials. These are materials that are anticipated to have high molecular second-order polarizability, β, which will contribute to the field-induced dipole moment. Extensive research has been done on identifying organic molecules that may possess large second-order polarizabilities based on this simple criterion, while organometallic molecules remain virtually unexplored.[3]

However, use of molecules that possess high molecular second-order hyperpolarizabilites, β, does not guarantee their usefulness for second harmonic generation. Because the field strength is a vector, the field-induced molecular polarization and the bulk second-order susceptibility ($\chi^{(2)}$) are not scalar. Second harmonic generation is measured on bulk samples that consist of ensembles of individual molecules. Bulk materials for second harmonic generation must be noncentrosymmetric; the material must crystallize in an acentric space group. Also, while there is not a one-to-one mapping between the molecular second-order term β and the bulk coefficient $\chi^{(2)}$, the most advantageous relationship between β and $\chi^{(2)}$ can be shown[4] to exist for polar molecules that crystallize in point groups 1, 2, m, or $mm2$. This is both an advantage and a disadvantage for chemists interested in optimum materials for second harmonic generation. The advantage is that it allows one to search crystal structure literature seeking molecules that are members of only several of many possible symmetry groups. This approach has been taken by Twieg[5] in a systematic search for suitable materials. The disadvantage of this approach is that it prevents the physical organic and organometallic chemist from choosing the optimum molecule (highest molecular polarizability), because it may or may not crystallize in an appropriate space group.

To date, methods for engineering small polar molecules into acentric environments have been restricted to thin-film (Langmuir–Blodgett monolayers,[6] orientation of molecules in polymer glasses[7] using strong electric or magnetic fields, or use of liquid-crystalline mesogens[6]) or directed crystal growth techniques.[8] The technique we have developed is one of dipolar alignment, in which a general, polarizable guest is inserted into an inclusion matrix host in a manner than enhances the probability of bulk acentric orientation. The initial work in this area by Eaton and Wang involved cyclodextrin complexation of nitroaniline derivatives as a method of inducing SHG activity in organic materials with inherently high β but vanishing $\chi^{(2)}$ because of the guests' centric crystal habits.[9] A similar approach was also reported by a Japanese group.[10]

We are interested in organometallics for nonlinear optics. Although organometallics have remained virtually unexplored for nonlinear optical applications, they should be capable of possessing large second-order polarizabilities on the basis of the simple criterion used for organics. In addition, organometallics have metal-to-ligand as well as ligand-to-metal charge-transfer states not available in organic systems.[11] Also, many organometallics contain π-conjugated systems, and one may use organometallic moieties to modify organic charge-transfer states.[3a,c]

We are also interested in exploring new methods of controlling molecular orientation so as to enhance the probability of obtaining an acentric structure. For molecules with ground-state dipoles, one would expect head-to-tail dipolar antiparallel pair formation to maximize electrostatic attraction. This major packing force is probably why most molecules prefer to pack in a centrosymmetric fashion.[12] In this study, we have determined that channel inclusion complexation is a viable method for dipolar alignment which enhances the chances for obtaining an acentric material suitable for SHG[13] and that bulk polar alignment can be obtained by using hosts that are not themselves chiral and thus naturally acentric. This is a significant finding which indicates that alignment in one channel need not be counterbalanced by antiparallel alignment in neighboring channels.

Experimental Section

General Procedures. Melting points were taken on a Thomas Hoover capillary apparatus and are uncorrected. IR spectra were

(1) (a) Gedanken, A.; Robb, M. B.; Keubler, N. A. *J. Phys. Chem.* **1982**, *86*, 4096. (b) *Nonlinear Optical Properties of Organic and Polymeric Materials*; Williams, D. J., Ed.; ACS Symposium Series No. 233; American Chemical Society: Washington, D.C., 1983. (c) Williams, D. J. *Angew. Chem., Int. Ed. Engl.* **1984**, *23*, 690. (d) Basu, S. *Ind. Eng. Chem. Prod. Res. Dev.* **1984**, *23*, 183. (e) Glass, A. M. *Science* **1984**, *226*, 657. (f) *Nonlinear Optical Properties of Organic Molecules and Crystals*; Chemla, D. S., Zyss, J., Eds.; Academic Press: New York, 1987; Vol. 1 and 2.

(2) Oudar, J. L.; Chemla, D. S. *J. Chem. Phys.* **1977**, *66*, 2664.

(3) Reference on organometallics for nonlinear optics: (a) Tam, W.; Calabrese, J. C. *Chem. Phys. Lett.* **1988**, *144*, 79. (b) Calabrese, J. C.; Tam, W. *Chem. Phys. Lett.* **1987**, *133*, 244. (c) Green, M. L. H.; Marder, S. R.; Thompson, M. E.; Bandy, J. A.; Bloor, D.; Kolinsky, P. V.; Jones, R. J. *Nature* **1987**, *26*, 360. (d) Frazier, C. C.; Harvey, M. A.; Cockerham, M. P.; Hand, H. M.; Chauchard, E. A.; Lee, C. H. *J. Phys. Chem.* **1986**, *90*, 5703. Frazier, C. C.; Guha, S.; Chen, W. P.; Cockerham, M. P.; Porter, P. L.; Chauchard, E. A.; Lee, C. H. *Polymer* **1987**, *28*, 553.

(4) Oudar, J. L.; Zyss, J. *Phys. Rev.* **1982**, *A26*, 2016, 2028.

(5) (a) Jain, K.; Crowley, J. J.; Hewig, G. H.; Cheng, Y. Y.; Twieg, R. *Opt. Laser Technol.* **1981**, *13*, 297. (b) Twieg, R.; Azema, A.; Jain, K.; Cheng, Y. Y. *Chem. Phys. Lett.* **1982**, *92*, 208.

(6) Garito, A. F.; Singer, K. D.; Teng, C. C. In *Nonlinear Optical Properties of Organic and Polymeric Materials*; Williams, D. J., Ed.; ACS Symposium Series No. 233; American Chemical Society: Washington, D.C., 1983; p 1.

(7) (a) Meredith, G. R.; Van Duesen, J. G. In *Nonlinear Optical Properties of Organic and Polymeric Materials*; Williams, D. J., Ed.; ACS Symposium Series No. 233; American Chemical Society: Washington, D.C., 1983; p 120. (b) Sohn, J. E.; Singer, K. D.; Lalama, S. J.; Kuzyk, M. G. *Polym. Mater. Sci. Eng.* **1986**, *55*, 532. (c) Ye, C.; Marks, T. J.; Yang, J.; Wong, G. K. *Macromolecules* **1987**, *20*, 2322.

(8) Addadi, L.; Berkovitch-Yellin, Z.; van Mil, J.; Shimon, L. J. W.; Lahav, M.; Leiserowitz, L. *Angew. Chem., Int. Ed. Engl.* **1985**, *24*, 466.

(9) Wang, Y.; Eaton, D. F. *Chem. Phys. Lett.* **1985**, *120*, 441.

(10) Tomaru, S.; Zembutsu, S.; Kawachi, M.; Kobayashi, M. *J. Chem. Soc., Chem. Commun.* **1984**, 1207.

(11) Geoffroy, G. L.; Wrighton, M. S. *Organometallic Photochemistry*; Academic Press: New York, 1979.

(12) Nicoud, J. F.; Twieg, R. J. In *Nonlinear Optical Properties of Organic Molecules and Crystals*; Chemla, D. S., Zyss, J., Eds.; Academic Press: New York, 1987; Vol. 1, p 227.

(13) Preliminary communications of this work have been published: (a) Anderson, A. G.; Calabrese, J. C.; Tam, W.; Williams, I. D. *Chem. Phys. Lett.* **1987**, *134*, 392. (b) Eaton, D. F.; Anderson, A. G.; Tam, W.; Wang, Y. *J. Am. Chem. Soc.* **1987**, *109*, 1886. (c) Eaton, D. F.; Anderson, A. G.; Tam, W.; Wang, Y. In *Polymers for High Technology Electronics and Photonics*; Bowden, M. J., Turner, R. S., Eds.; ACS Symposium Series No. 346; American Chemical Society: Washington, D.C., 1987; p 381.

recorded on a Perkin-Elmer 9830 spectrophotometer. ^1H and ^{13}C NMR spectra were performed on a QE-300 Nicolet spectrometer. Elemental analyses were performed by Schwarzkopf Microanalytical laboratory, Woodside, NY, and Micro-analysis Inc., Wilmington, DE. Methanol was degassed by purging with nitrogen and stored under molecular sieves (4A) in the drybox. Benzene, hexane, pentane, tetrahydrofuran (THF), diethyl ether, and toluene were purified by distillation from purple sodium/benzophenone ketyl solutions under nitrogen. Methylene chloride was dried over phosphorus pentoxide and degassed by purging with nitrogen. Deuterated solvents were dried and degassed analogously to their protonated counterparts. The following were prepared by literature procedures: (η^6-fluorobenzene)$Cr(CO)_3$, (η^6-indan)$Cr(CO)_3$, (η^6-anisole)$Cr(CO)_3$, (η^6-(dimethylamino)-benzene)$Cr(CO)_3$, (η^6-*cis*-stilbene)$Cr(CO)_3$, (η^6-*trans*-stilbene)-$Cr(CO)_3$,[14] (η^4-trimethylenemethane)$Fe(CO)_3$,[15] (η^5-CpCr$(CO)_2$-(NO)[16] (Cp = cyclopentadienyl), (η^5-cyclohexadienyl)$Mn(CO)_3$,[17] η^5-CpRe$(CO)_3$,[18] (η^4-pyrrolyl)$Mn(CO)_3$,[19] (η^4-thiophene)$Cr(CO)_3$,[20] (η^4-1,3-cyclohexadiene)RhCp,[21] η^5-CpRh$(ethylene)_2$,[22] (η^4-1,3-cyclohexadiene)CoCp,[23] (η^5-Cp$)_2WH_2$,[24] [(η^6-benzene)$Mn(CO)_3$]-BF_4,[14] and $W(CO)_5$(4-X-pyridine) (X = H, NH_2, CH_3, CH_2CH_3).[25] (η^6-Benzene)$Cr(CO)_3$, (η^6-tetralin)$Cr(CO)_3$, $CpMn(CO)_3$, (η^4-1,3-cyclohexadiene)$Fe(CO)_3$, and (η^4-butadiene)$Fe(CO)_3$ were obtained commerically.

Preparation of Tris-*o*-thymotide. This procedure is a modification of several literature preparations.[26] In the drybox, a 500-mL round-bottom flask with a sidearm was charged with 40 g of *o*-thymotic acid,[27] 19 mL of phosphorus oxychloride, and 250 mL of xylene. The mixture was taken out of the drybox and heated under nitrogen at 110 °C in an oil bath overnight. The resultant dark brown mixture was cooled in an ice bath, and 60 mL of water added. The organic layer was separated and dried over $MgSO_4$. The solvent was removed by rotary evaporation, and 200 mL of ethanol was added. The mixture was refluxed for 20 min and then decanted hot. The insoluble material was dissolved in hot ethanol (about 250–300 mL), and the solution filtered hot. Both extracts were cooled to room temperature and allowed to set overnight. The solid that crystallizes from the second EtOH wash should be pure TOT/ethanol inclusion compound (up to 8.9 g). This was recrystallized from hot heptane. The solid from the first EtOH wash was a mixture of TOT and an impurity. Pure TOT was obtained from this mixture after flash column chromatography, eluted with $CHCl_3$. The impurity eluted first followed by TOT. The TOT (about 5 g) from this column was recrystallized from hot heptane. The pure TOT/heptane inclusion material was combined and vacuum dried initially at 130 °C for 4 h and then at 150 °C overnight. Drying was then continued at 160 °C until all of the included heptane was removed. Pure TOT melts at 216 °C.

General Procedures for Preparing Inclusion Compounds. A. About 200–500 mg of an organometallic complex was added to about 15–20 mL of a 50% saturated solution of thiourea in methanol. The mixture was heated if necessary to dissolve the organometallic complex, and the solution filtered under pressure. Crystals formed upon slow cooling from about 0 °C to about −20 °C.

B. Alternatively, thiourea and the organometallic complex in a ratio of about 3:1 were dissolved in methanol, followed by removal of the solvent under reduced pressure. The solid isolated from this simple procedure provided material suitable for SHG measurements. The SHG measurements obtained for [(thiourea)$_3$·(η^6-benzene)$Cr(CO)_3$] prepared in this manner were very close to those obtained from samples prepared by method A (2 × urea).

C. A mixture of about 150 mg of tris-*o*-thymotide (TOT) in about 50 mL of methanol was heated until the TOT dissolved and then allowed to cool to room temperature. About 150 mg of the guest molecule was added to the TOT/methanol solution, and the mixture was heated if necessary to dissolve the guest compound. The solution was filtered under pressure at room temperature, and the methanol allowed to evaporate slowly at room temperature. Upon concentration, crystals of the inclusion compound formed and were isolated by filtration.

In the preparations described below using method A or C, nice crystals of the inclusion complexes generally formed in preference to crystallization of the host or guest. ^1H NMR spectra of the thiourea inclusion complexes in deuterated methanol and ^1H NMR spectra of the TOT inclusion complexes in deuterated methylene chloride were taken to verify that the organometallics had remained unreacted. In some cases, mixtures were obtained that could not be separated, and therefore the host:guest ratio could not be determined. ^1H NMR spectra of these mixtures indicated the presence of the host and guest. The SHG activity of these mixtures attests to the fact that the inclusion compound had indeed formed. For some thiourea examples, crystals of the inclusion compound can be separated by hand from cocrystallized thiourea.

Preparation of Thiourea Inclusion Compounds. (η^6-Benzene)$Cr(CO)_3$. The procedure described in method A was followed using 15 mL of thiourea solution and 250 mg of (η^6-benzene)$Cr(CO)_3$. After 2 days at 0 °C, yellow needles were isolated: mp 158–170 °C (decomp); IR (KBr) 1948 s, 1892 m, 1879 s, 1848 w, 1632 w, 1615 m, 1490 w cm^{-1}. Anal. Calcd for $C_{12}H_{18}CrN_6O_3S_3$: C, 32.57; H, 4.10; Cr, 11.75. Found: C, 32.72; H, 4.18; Cr, 11.29. In a larger scale preparation, 2 g of (η^6-benzene)$Cr(CO)_3$ was dissolved in 200 mL of 50% saturated thiourea solution in methanol, and the mixture was filtered under pressure. The mixture was then kept at 0 °C for several days. The crystals were filtered, washed with cold methanol, and dried to give 2.124 g (4.8 mmol, 51% based on the amount of (η^6-benzene)$Cr(CO)_3$ used) of the inclusion compound. Crystals obtained were suitable for X-ray structural analysis.

(η^6-Fluorobenzene)$Cr(CO)_3$. The procedure described in method A was followed using 15 mL of thiourea solution and 250 mg of (η^6-fluorobenzene)$Cr(CO)_3$. Cooling to −20 °C yielded yellow needles of the inclusion complex, which were separated by hand from crystals of thiourea: IR (KBr) 1958 vs, 1932 w, 1892 vs, 1632 s, 1489 m, 1461 m cm^{-1}. Anal. Calcd for $C_{12}H_{17}CrFN_6O_3S_3$: C, 31.30; H, 3.72; Cr, 11.29. Found: C, 31.13; H, 3.88; Cr, 11.13.

(η^4-1,3-Cyclohexadiene)$Fe(CO)_3$. The procedure described in method A was followed using 300 mg of (η^4-1,3-cyclohexadiene)$Fe(CO)_3$ and 15 mL of the thiourea solution. Cooling to −20 °C yielded 244 mg of yellow needles: IR (KBr) 2043 s, 1964 s, 1957 sh, 1613 s. Anal. Calcd for $C_{12}H_{20}FeN_6O_3S_3$: C, 32.15; H, 4.50; Fe, 12.46. Found: C, 32.01; H, 4.47; Fe, 12.60. Crystals obtained were suitable for X-ray structural analysis.

(η^5-Cyclohexadienyl)$Mn(CO)_3$. Method A was followed using 400 mg of η^5-(cyclohexadienyl)$Mn(CO)_3$ and 15 mL of thiourea solution and −20 °C temperature gave 188 mg of the inclusion complex: IR (KBr) 2006 s, 1945 sh, 1931 s, 1919 s, 1633 w, 1615 s cm^{-1}. Anal. Calcd for $C_{12}H_{19}MnN_6O_3S_3$: C, 32.28; H, 4.29. Found: C, 32.11; H, 4.43. Crystals were suitable for X-ray analysis.

(η^4-Trimethylenemethane)$Fe(CO)_3$. Method A was used with 300 mg of η^4-(trimethylenemethane)$Fe(CO)_3$ and 15 mL of the thiourea solution at −18 °C. Long, thin, and very pale yellow needles of the inclusion complex were isolated: IR (KBr) 2060 m, 1986 s, 1613 s. Anal. Calcd for $C_{10}H_{18}FeN_6O_3S_3$: C, 28.44; H, 4.30; Fe, 13.22. Found: C, 28.36; H, 4.33; Fe, 12.79.

(14) Mahaffy, C. A. L.; Pauson, P. L. *Inorg. Synth.* **1979**, *19*, 154.
(15) Emerson, G. F.; Ehrlich, K.; Giering, W. P.; Lauterbur, P. C. *J. Am. Chem. Soc.* **1966**, *88*, 3172.
(16) Hoyano, J. K.; Legzdins, P.; Malito, J. T. *Inorg. Synth.* **1978**, *18*, 126.
(17) Winkhaus, G.; Pratt, L.; Wilkinson, G. *J. Chem. Soc.* **1961**, 3808.
(18) Tam, W.; Lin, G. Y.; Wong, W. K.; Kiel, W. A.; Wong, V. K.; Gladysz, J. A. *J. Am. Chem. Soc.* **1982**, *104*, 141.
(19) Joshi, K. K.; Pauson, P. L.; Quzi, A. R.; Stubbs, W. H. *J. Organomet. Chem.* **1964**, *1*, 471.
(20) Novi, M.; Guanti, G.; Dell'Erba, C. *J. Heterocycl. Chem.* **1975**, *12*, 1055.
(21) Johnson, B. F. G.; Lewis, J.; Yarrow, D. J. *J. Chem. Soc., Dalton Trans.* **1972**, 2084.
(22) King, R. B. *Inorg. Chem.* **1963**, *2*, 528.
(23) Lai, Y. H.; Tam, W.; Vollhardt, K. P. C. *J. Organomet. Chem.* **1981**, *216*, 97.
(24) Green, M. L. H.; McCleverty, J. A.; Pratt, L.; Wilkinson, G. *J. Chem. Soc.* **1961**, 4854.
(25) Wrighton, M. S.; Abrahamson, H. B.; Morse, D. L. *J. Am. Chem. Soc.* **1976**, *98*, 4104.
(26) Arad-Yellin, R.; Brunie, S.; Green, B. S.; Knossow, M.; Tsoucaris, G. *J. Am. Chem. Soc.* **1979**, *101*, 7529, and references therein.
(27) Street, J. P.; George, C. E.; Jannke, P. J. *Bull. Soc. Chim. Fr.* **1955**, 1421.

η^5-CpMn(CO)$_3$. Method A was used with 500 mg of η^5-CpMn(CO)$_3$ and 10 mL of the thiourea solution. After cooling to 0 °C for about 4 days, 230 mg of crystals were obtained: IR (KBr) 2112 s, 2006 sh, 1954 w, 1927 vs, 1634 w, 1616 s, 1490 w cm^{-1}. Anal. Calcd for $C_{11}H_{17}MnN_6O_3S_3$: C, 30.55; H, 3.96. Found: C, 30.74; H, 4.25.

η^5-CpRe(CO)$_3$. The procedure described in method B was followed using 100 mg of η^5-CpRe(CO)$_3$ and 100 mg of thiourea in 15 mL of methanol. SHG: 0.5 × urea.

(η^4-Butadiene)Fe(CO)$_3$. Method A was used with 400 mg of (η^5-butadiene)Fe(CO)$_3$ and 10 mL of thiourea solution. After 2 days at −15 °C, 129 mg of light yellow crystals was isolated. The product turned white over a period of a week; this suggested that the guest compound was coming out of the channels. This complex was also prepared by method B; 100 mg of (η^4-butadiene)-Fe(CO)$_3$ and 120 mg of thiourea were dissolved in 15 mL of MeOH. After removal of solvent, the residue generated SHG with relative efficiency comparable to urea.

(η^4-Pyrrolyl)Mn(CO)$_3$. Method B was followed using 100 mg of (η^4-pyrrolyl)Mn(CO)$_3$ and 100 mg of thiourea in 15 mL of MeOH to give a yellow solution from which the inclusion complex was obtained.

η^5-CpCr(CO)$_2$NO. Method A was used with 400 mg of η^5-CpCo(CO)$_2$NO and 15 mL of the thiourea solution. After about 2 weeks at 0 °C, fiberlike needles were isolated: IR (KBr) 2019 sh, 2011 s, 1941 m, 1700 m, 1615 s cm^{-1}. Anal. Calcd for $C_{10}H_{17}CrN_7O_3S_3$: C, 27.84; H, 3.97; Cr, 12.05. Found: C, 27.80; H, 3.95; Cr, 12.30.

(η^4-Thiophene)Cr(CO)$_3$. Method B was used with 100 mg of (thiophene)Cr(CO)$_3$ and 100 mg of thiourea in 15 mL of MeOH.

(η^4-1,3-Cyclohexadiene)RhCp. Method A was followed using 200 mg of (1,3-cyclohexadiene)RhCp. Thin yellow crystals were obtained after cooling to 0 °C. Anal. Calcd for $C_{15}H_{29}N_8S_4Rh$ (4 thiourea:1 (1,3-cyclohexadiene)RhCp): C, 32.60; H, 5.29; Rh, 18.62. Found: C, 33.06; H, 5.59; Rh, 14.42, 14.75. The C and H analyses were within the calculated range, but the Rh was not. A MAS ^{13}C spectrum was obtained: 82.0, 75.5, 54.7, 29.4, and 25.8 ppm. For comparison, a ^{13}C NMR spectrum of (1,3-cyclohexadiene)RhCp in THF-d_8 was taken: 83.2 (d, J = 5 Hz), 76.5 (d, J = 7.5 Hz), 55.8 (d, J = 16 Hz), and 27.6 (s) ppm.

η^5-CpRh(η^2-ethylene)$_2$. Method A was used with 100 mg of η^5-CpRh(η^2-ethylene)$_2$ in 7 mL of thiourea solution in methanol. The mixture was cooled to −15 °C. Anal. Calcd for $C_{12}H_{25}N_6S_3Rh$ (3 thiourea: 1 η^5-CpRh(η^2-ethylene)$_2$): C, 31.85; H, 5.57; Rh, 22.74. Found: C, 31.54, 31.82; H, 5.71, 5.45; Rh, 22.86. This material was found to be SHG inactive.

(η^4-1,3-Cyclohexadiene)Co(η^5-Cp). Method A was used with 250 mg of (η^4-1,3-cyclohexadiene)CoCp and 15 mL of thiourea solution. After several days at 0 °C, 313 mg of orange crystals was isolated. Anal. Calcd for $C_{15}H_{29}S_4N_8Co$ (4 thiourea:(η^4-1,3-cyclohexadiene)Co(η^5-Cp)): C, 35.42; H, 5.75; Co, 11.59. Found: C, 36.02, 35.75; H, 5.89, 5.67; Co, 11.78, 11.50, 12.39. This material was found to be SHG inactive.

(η^5-Cp)$_2$WH$_2$. Method A was used with 250 mg of (η^5-Cp)$_2$WH$_2$. After cooling at 0 °C for several days, 296 mg of yellow crystals were collected. Anal. Calcd for $C_{13}H_{24}N_6S_3W$: C, 28.68; H, 4.44; W, 33.77. Found: C, 29.14; H, 4.69; W, 33.92.

Preparation of TOT Complexes. (η^6-Indan)Cr(CO)$_3$. Method C was used with 250 mg of the organometallic to give 157 mg of the inclusion compound: IR (KBr) 1958 s, 1874 s, 1765 m, 1269 w, 1257 w, 1219 m, 1092 m. Anal. Calcd for $C_{45}H_{46}CrO_9$: C, 69.04; H, 5.92. Found: C, 68.97; H, 5.71.

(η^6-Anisole)Cr(CO)$_3$. Method C was used with 250 mg of the organometallic compound to give 160 mg of the inclusion compound: IR (KBr) 1963 s, 1878 s, 1764 m, 1269 w, 1256 w, 1220 m, 1092 m. Anal. Calcd for $C_{43}H_{44}O_{10}Cr$: C, 68.24; H, 5.86. Found: C, 67.62; H, 5.63.

(η^6-Tetralin)Cr(CO)$_3$. Method C was followed using 300 mg of (tetralin)Cr(CO)$_3$; 110 mg of yellow crystals were obtained and were suitable for X-ray structural analysis. Anal. Calcd for $C_{46}H_{48}O_9Cr$: C, 69.33; H, 6.07. Found: C, 68.89; H, 6.00. IR (KBr) 1957 s, 1872 s, 1765 m, 1269 w, 1257 w, 1220 m, 1092 m.

[(η^6-Benzene)Mn(CO)$_3$]BF$_4$. Method C was followed using 300 mg of the organometallic. Evaporation of some of the solvent produced a mixture most likely consisting of TOT, starting organometallic, and the inclusion complex. It was difficult to separate the inclusion compound from this mixture, and the SHG powder measurement was measured with this mixture.

(η^6-(Dimethylamino)benzene)Cr(CO)$_3$. Method C was followed using 250 mg of the organometallic. Heating was needed to dissolve the organometallic. Nice yellow needles were obtained (185 mg): IR (KBr) 1951 vs, 1857 vs, 1764 s, 1551 m, 1487 w, 1220 s, 1092 m. Anal. Calcd for $C_{44}H_{47}O_9NCr$: C, 67.25; H, 6.03. Found: C, 67.06; H, 5.81.

(*p*-Cyanobenzoyl)Mn(CO)$_5$. Method C was followed using 150 mg of (*p*-cyanobenzoyl)Mn(CO)$_5$ to give a mixture containing the inclusion compound. The starting organometallic was prepared by treating NaMn(CO)$_5$ (generated from $Mn_2(CO)_{10}$ and Na amalgam) with 4-cyanobenzoyl chloride in THF at −78 °C. The product was purified by recrystallization from ether: ^{1}H NMR (CD_2Cl_2) 7.67 (d, J = 8 Hz, 2 H), 7.34 (d, J = 8 Hz, 2 H); IR (THF) 2225 w, 2120 m, 2022 vs, 1580 m. Anal. Calcd for $C_{14}H_4O_6NMn$: C, 48.03; H, 1.24. Found: C, 48.20; H, 1.44.

(η^6-*trans*-Stilbene)Cr(CO)$_3$. TOT (50 mg) was dissolved in 15 mL of hot MeOH. After cooling to room temperature, the solution was filtered into a flask containing 50 mg of (η^6-*trans*-stilbene)Cr(CO)$_3$. Orange crystals were obtained after allowing the solution to evaporate. Anal. Calcd for $C_{50}H_{48}O_9Cr$: C, 71.08; H, 5.73. Found: C, 71.02; H, 5.69. This material was found to be SHG inactive.

(η^6-*cis*-Stilbene)Cr(CO)$_3$. Method C was used with 150 mg of η^6-(*cis*-stilbene)Cr(CO)$_3$ as guest. After evaporation of some of the solvent, crystals were obtained. This material was SHG inactive.

***trans*-*p*-(Dimethylamino)cinnamaldehyde.** Method C was used with 200 mg of *trans*-*p*-(dimethylamino)cinnamaldehyde. Anal. Calcd for $C_{77}H_{85}NO_{13}$: C, 75.03; H, 6.95. Found: C, 74.81; H, 6.82. SHG of this material was 0.06 × urea. This complex was also prepared by adding a 50-mL methanol solution containing 150 mg TOT to 10 mL of hot methanol containing 200 mg of *trans*-*p*-(dimethylamino)cinnamaldehyde. The solution was cooled to room temperature and then cooled to 0 °C. After 7 days, 90 mg (mp 217–218 °C) of light orange–yellow rhombohedral crystals were separated by hand from about 5–10 mg of fibrous crystals. This material has SHG activity of 0.3–1.0 × urea. Both set of crystals were submitted for X-ray structural studies, and both yielded the same disordered structure.

***p*-(Dimethylamino)benzonitrile.** Method C was followed using 150 mg of *p*-(dimethylamino)benzonitrile; 90 mg of white crystals were isolated. Anal. Calcd for $C_{75}H_{82}N_2O_{12}$: C, 74.85; H, 6.87. Found: C, 74.91; 74.66; H, 6.56, 6.56. Elemental analyses could not be used to distinguish a 2:1 host-to-guest complex from a 1:1 host-to-guest complex. The ^{1}H NMR (CD_2Cl_2) spectrum determined that this was a 2:1 host-to-guest complex.

W(CO)$_5$(pyridine). Method C was followed using 200 mg of W(CO)$_5$(pyridine). After some of the solvent was allowed to evaporate, 168 mg of yellow crystals was obtained: IR (KBr) 2071 w, 1976 w, 1929 vs, 1898 sh, 1765 s, 1219 s, 1092 s. Anal. Calcd for $C_{78}H_{85}O_{19}NW$: C, 61.46; H, 5.62; W, 12.06. Found: C, 62.03; H, 5.47; W, 11.61. Large crystals were obtained and were suitable for X-ray structural analysis.

W(CO)$_5$(4-aminopyridine). Method C was used with 200 mg of W(CO)$_5$(4-aminopyridine). Collected was 160 mg of yellow crystals: IR (KBr) 2068 w, 1937 s, 1904 s, 1879 s, 1761 s, 1734 m, 1633 m, 1609 w, 1217 s, 1093 m. Anal. Calcd for $C_{78}H_{86}O_{19}N_2W$: C, 60.86; H, 5.63; W, 11.94. Found: C, 60.96, 61.11; H, 5.78, 5.63; W, 11.62, 11.88. Crystals were suitable for X-ray structural analysis.

W(CO)$_5$(4-picoline). Method C was followed using 150 mg of W(CO)$_5$(4-picoline). Collected was 169 mg of yellow crystals: IR (KBr) 2070 w, 1980 w, 1921 s, 1892 m, 1762 m, 1220 m, 1093 m. Anal. Calcd for $C_{44}H_{43}O_{11}NW$: C, 55.88; H, 4.58; W, 19.44. Found: C, 55.65; H, 4.72; W, 18.96. Crystals were suitable for X-ray structural analysis.

W(CO)$_5$(4-ethylpyridine). Method C was used with 200 mg of W(CO)$_5$(4-ethylpyridine). Collected was 147 mg of yellow crystals: IR (KBr) 2071 w, 1977 m, 1921 s, 1910 s, 1897 sh, 1764 m, 1220 s, 1092 m. Anal. Calcd for $C_{45}H_{45}O_{11}NW$: C, 56.32; H, 4.73. Found: C, 56.85, 56.74; H, 4.69, 4.70. Crystals were suitable for X-ray structural analysis.

X-ray Structural Analyses. Data were collected on either a Syntex R3 or an Enraf-Nonius CAD4 diffractometer, with

graphite-monochromated Mo Kα radiation. Structures were refined by Patterson (PHASE) methods or by direct methods (MULTAN).

Method of Measuring SHG. SHG measurements were made with a modification of the method of Kurtz and Perry,[28] using powder samples (250-mm-thick cell). Urea (63–90 μm) was used as a reference material.[29] A Nd:YAG laser is directed through an optical neutral density filter to adjust the light intensity. The beam then passes through a hole in a parabolic mirror and illuminates a sample. Light emerging from the sample is collected by the mirror and passed through a beam splitter. One portion of the signal is passed through an optical narrow band-pass filter (fwhm 10 nm) which passes light at the second harmonic frequency only (532 nm). The second portion passes through another filter which is a broad-band filter (fwhm 70 nm). Each portion of the split beam is detected with photomultipliers. The detected signals are compared electronically. Thus in each experiment, two-channel detection is employed to discriminate against spurious signals (fluorescence or scattered light) that can be generated. No effort was made during this study to examine any of the materials for phase-matchability. Samples were crushed to a fine powder with a mortar and pestle; no particle size classification was done. Errors in SHG signal intensities can in principle be quite large since grain size differences are not taken into account.

Results and Discussion

In this paper, we provide full experimental and structural details on our work on the use of channel inclusion complexation for dipolar alignment of organometallics for preparation of materials suitable for SHG. We have used thiourea and tris-*o*-thymotide (TOT) as hosts in this study because they are well-known to form channel inclusion complexes.[30] Choices of appropriate guests are limited to those molecules that cocrystallize as inclusion compounds with the selected hosts. Many factors contribute to determine if an inclusion compound can be formed. Some practical considerations are (1) solubility of the host and guest in a common solvent, (2) size and shape restriction of the guest as determined by the size and shape of the channels, and (3) relative propensity for inclusion of the solvent versus inclusion of the desired guest. In addition to these restrictions on the choice of suitable guests for our use we require that the guest should possess a molecular second-order hyperpolarizability. In the absence of measured values for β, we have chosen organometallics that possess low-lying charge-transfer (CTML or CTLM) excited states in their excited-state manifold to ensure this latter requirement within the paradigm of the two-state model.[2] Finally, all the precursors we employ for preparation of inclusion compounds reported here are all centrosymmetric in their normal native crystal forms, so that all are incapable of SHG themselves.

Thiourea Inclusion Complexation of Organometallics. The inclusion compound of ferrocene with thiourea has been reported.[31] We decided to try to include (η^6-benzene)$Cr(CO)_3$ with thiourea because it is about the same size as ferrocene and it should possess a moderate molecular second-order hyperpolarizability since its absorption spectrum is dominated by metal-to-ligand charge-transfer absorptions.[11]

(28) Kurtz, S. K.; Perry, T. T. *J. Appl. Phys.* **1968**, *89*, 8798.
(29) (a) Betzer, H.; Hesse, H.; Loose, P. *J. Mol. Struct.* **1978**, *47*, 393. (b) Halbout, J. L.; Blit, S.; Donaldson, W.; Tang, C. L. *IEEE J. Quantum Electron.* **1979**, *QE*-15, 1176. (c) Cassidy, C.; Halbout, J. M.; Donaldson, W.; Tang, C. L. *Opt. Commun.* **1979**, *29*, 243.
(30) *Inclusion Compounds*; Atwood, J. L., Davies, J. E. D., MacNicol, D. D., Eds.; Academic Press: New York, 1984; Vol. 2, Chapter 2.
(31) (a) Houg, E.; Nicholson, D. G. *J. Chem. Soc., Dalton Trans.* **1978**, *15*. (b) Nakai, T.; Terao, T.; Imashiro, F.; Saika, A. *Chem. Phys. Lett.* **1986**, *132*, 554. (c) Bozak, R. E.; Barone, A. D. *Chem. Lett.* **1975**, *75*. (d) Clement, R.; Claude, R.; Mazieres, C. *J. Chem. Soc., Chem. Commun.* **1974**, 654.

Table I. Crystal Data and Summary of Intensity Data Collection and Structure Refinement for Thiourea Inclusion Complexes 1–4

	1	2	3	4
mol wt	442.51	448.37	422.33	447.46
space group	*R3c*	*Pna2*$_1$	*R3c*	*R3c*
cell consts				
a, Å	16.130 (5)	12.562 (1)	16.234 (2)	16.307 (2)
b, Å	16.130 (5)	16.128 (1)	16.234 (2)	16.307 (2)
c, Å	12.569 (5)	9.536 (1)	12.488 (3)	12.653 (2)
α, deg	90.0	90.0	90.0	90.0
β, deg	90.0	90.0	90.0	90.0
γ, deg	120.0	90.0	120.0	120.0
cell vol, Å^3	2832.0	1932.0	2850.2	2913.9
molecules/unit cell	6	4	6	6
D(calcd), g cm^{-3}	1.556	1.541	1.476	1.530
temp, °C	−70	−100	−70	−100
μ(Mo)	9.33	11.14	11.28	9.85
2θ range, deg	4.4–55.0	4.1–55.0	4.4–55.0	4.3–54.9
total unique data	3969	2582	1845	1681
unique data with $I \geq 3\sigma(I)$	660	2082	646	605
no. of parameters varied	99	225	93	75
R	0.030	0.027	0.021	0.045
R_w	0.031	0.032	0.024	0.054

Table II. Selected Interatomic Distances (angstroms) and Intramolecular Angles (degrees) for 1

Cr(1)–C(1)	1.840 (4)	Cr(1)–C(2)	2.211 (4)
Cr(1)–C(3)	2.211 (5)	S(1)–C(4)	1.720 (4)
O(1)–C(1)	1.155 (6)	N(1)–C(4)	1.321 (6)
N(2)–C(4)	1.312 (7)	C(2)–C(3)b	1.393 (7)
C(2)–C(3)	1.407 (7)		
Cr(1)–C(1)–O(1)	179.2 (3)	Cr(1)–C(2)–H(2)	124 (3)
S(1)–C(4)–N(1)	121.0 (4)	S(1)–C(4)–N(2)	119.9 (4)
N(1)–C(4)–N(2)	119.0 (4)	C(3)–C(2)–C(3)b	119.7 (6)
C(2)–C(3)–C(2)a	120.3 (6)		

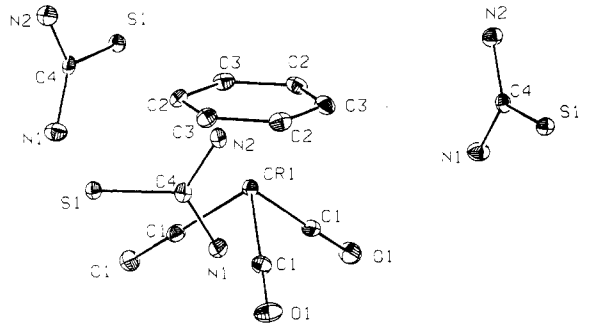

Figure 1. ORTEP of thiourea·(η^6-benzene)$Cr(CO)_3$ (**1**).

Crystals of the inclusion complex (thiourea)$_3$·(η^6-benzene)$Cr(CO)_3$ (**1**) were prepared by cocrystallization of the components. Powder measurements indicated the complex was capable of SHG with an efficacy about 2× that of urea, a common standard. Crystals of **1** suitable for X-ray structural studies were grown from 50% saturated thiourea solutions in methanol containing the organometallic at 0 °C. Combustion analysis and NMR studies show this to be a 3:1 host-to-guest inclusion complex. X-ray data for **1** indicate that the thiourea lattice is similar to that determined for the thiourea–ferrocene inclusion complex.[31] Crystallographic data and selected bond distances and angles are listed in Tables I and II (atomic coordinates and other data are presented in supplementary material (see the paragraph at the end of the paper)). The organometallic fragment is not structurally perturbed by inclusion: bond angles and distances are nearly identical with the free guest. The three thioureas are also unperturbed. They are related crystallographically by a 3-fold axis (Figure 1). Looking down the channel,

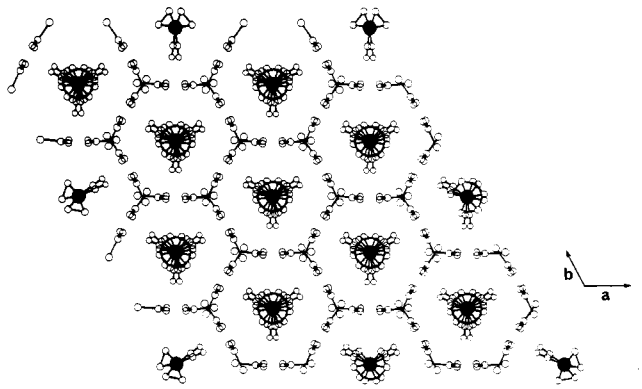

Figure 2. View down the channels of 1. Two (η^6-benzene)$Cr(CO)_3$ are shown in each channel for clarity.

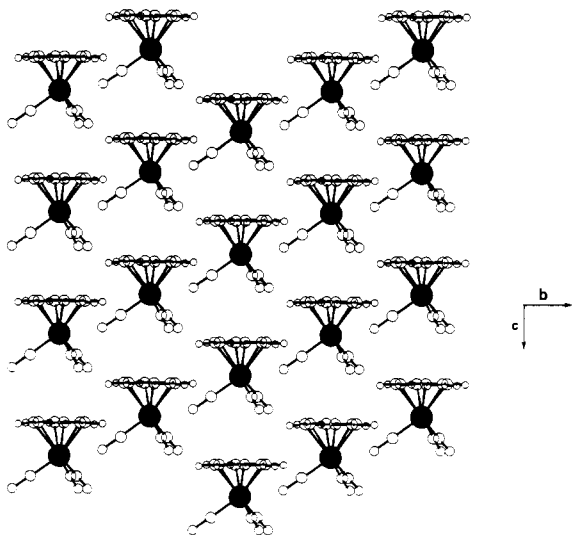

Figure 3. Arrangement of (η^6-benzene)$Cr(CO)_3$ in 1. Thioureas are deleted for clarity. Thioureas form channels running along the *c* axis.

one sees a hexagonal array of thioureas (Figure 2). The internal diameter of these channels is about 9.3 Å. The guest molecules stack along the axes of the channels with a separation of 2.8 Å between the planes formed by the carbonyl oxygens of one guest and the benzene ring of an adjacent guest. Each guest molecule is staggered by 13.3° from neighboring (η^6-benzene)$Cr(CO)_3$ molecules along the channel. Adjacent columns of (η^6-benzene)$Cr(CO)_3$ molecules are staggered to minimize head-to-head electrostatic repulsion. Electrostatic communication between columns must occur since all the (η^6-benzene)$Cr(CO)_3$ molecules are pointed in the same direction along the *c* axis (Figure 3).

The size of the channel is determined by hydrogen bonding between thioureas. One would expect the channel size to be inflexible due to optimization of this hydrogen bonding. The thioureas are arrayed in a tetragonal arrangement (Figure 4). Each sulfur is associated via H bonding with four adjacent NH_2 groups with S–N distances ranging from 3.4 to 3.5 Å. (η^6-Benzene)$Cr(CO)_3$ and ferrocene are the proper size to fit into these channels; any organometallics of similar size may be expected to form inclusion compounds with thiourea. This criterion guided our search for suitable guests. We have prepared several thiourea inclusion compounds. The SHG efficiencies at 1.06-μm laser light of the thiourea inclusion compounds are shown in Table III. All SHG values are listed relative to urea as a standard.

In general, these are 3:1 thiourea-to-organometallic inclusion complexes, and most of them generate SHG, indicating that most of them crystallize in acentric space groups. As expected, molecules about the size of (η^6-benzene)$Cr(CO)_3$ and ferrocene can be included. The benzene ligand can be replaced with Cp, diene, pyrrole, and thiophene, and the CO ligand can be replaced with NO. Unfortunately, because the thiourea channel size is inflexible and cannot be expanded, substituted (η^6-benzene)chromium tricarbonyls (except for (η^6-FC_6H_5)-$Cr(CO)_3$) cannot be included within thiourea. This size selectivity has allowed η^5-$CpMn(CO)_3$ to be separated from (acetyl)$CpMn(CO)_3$ and ferrocene to be separated from 1,1′-diethylferrocene by using inclusion complexation with thiourea.[32]

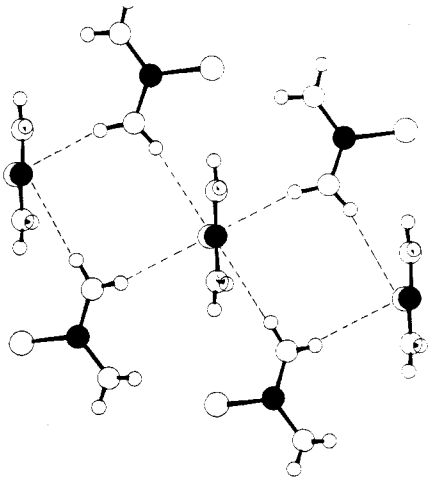

Figure 4. Tetragonal arrangement of thioureas in 1 due to hydrogen bonding.

Table III. Inclusion Complexes with Thiourea

guest	host:guest	SHG rel to urea
(η^6-benzene)$Cr(CO)_3$	3:1	2.3
(η^6-fluorobenzene)$Cr(CO)_3$	3:1	2.0
(η^4-1,3-cyclohexadiene)$Fe(CO)_3$	3:1	0.4
(η^4-trimethylenemethane)$Fe(CO)_3$	3:1	0.3
η^5-$CpMn(CO)_3$	3:1	0.3
η^5-$CpRe(CO)_3$	ND[a]	0.5
η^5-$CpCr(CO)_2(NO)$	3:1	0.1
(η^5-cyclohexadienyl)$Mn(CO)_3$	3:1	0.4
(η^4-1,3-butadiene)$Fe(CO)_3$	ND	1.0
(η^4-pyrrolyl)$Mn(CO)_3$	ND	0.2
(η^4-thiophene)$Cr(CO)_3$	ND	0.1
(η^4-1,3-cyclohexadiene)RhCp	4:1	0.0
η^5-$CpRh(ethylene)_2$	3:1	0.0
(η^4-1,3-cyclohexadiene)CoCp	4:1	0.0
$(\eta^5\text{-}Cp)_2WH_2$	3:1	0.0

[a] ND = not determined.

The structure of $(thiourea)_3$·(η^4-1,3-cyclohexadiene)$Fe(CO)_3$ (2) was determined. Unlike the $(thiourea)_3$·(η^6-benzene)$Cr(CO)_3$ structure, there are three unique thioureas for each (η^4-1,3-cyclohexadiene)$Fe(CO)_3$ (Figure 5). Crystal data and selected bond and angle parameters are listed in Tables I and IV. In this case, the organometallic guest stacks within the channels sideways as opposed to the perpendicular stacking observed in the previous structure of 1. The thiourea packing is again determined by hydrogen bonding, and the thioureas are again arranged in a tetragonal fashion. The iron-to-iron distance within a channel is 6.29 Å, and it is 9.46 Å across channels (about the same as the diameter of the channels). The arrangement is again polar, but the director of one layer of or-

(32) Nesmeyanov, A. N.; Shul'pin, G. B.; Rybinskaya, M. I. *Dokl. Chem.* **1975**, *221*, 229.

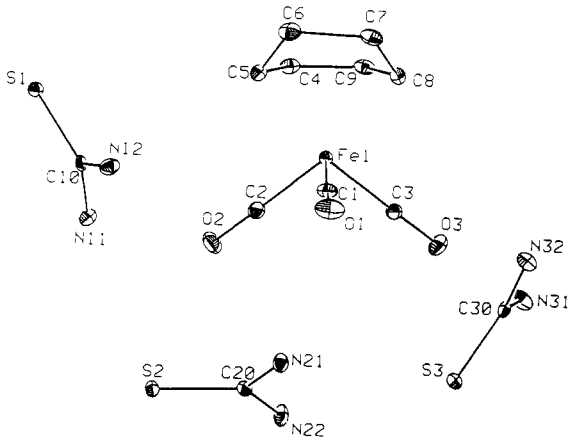

Figure 5. ORTEP of thiourea·(1,3-cyclohexadiene)$Fe(CO)_3$ (**2**).

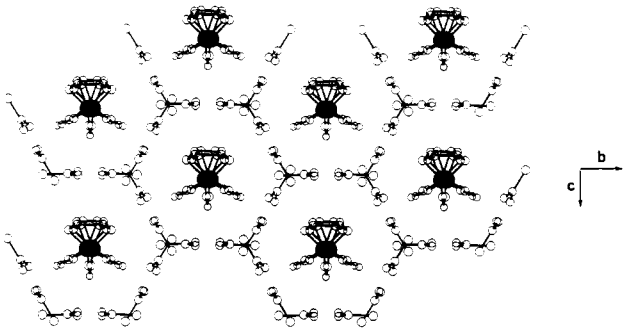

Figure 6. View down the channels of **2**. Two (η^4-1,3-cyclohexadiene)·$Fe(CO)_3$ in each channel are shown for clarity.

Table IV. Selected Interatomic Distances (angstroms) and Intramolecular Angles (degrees) for 2

Fe(1)–C(1)	1.799 (4)	Fe(1)–C(2)	1.798 (4)
Fe(1)–C(3)	1.794 (4)	Fe(1)–C(4)	2.030 (4)
Fe(1)–C(5)	2.104 (4)	Fe(1)–C(8)	2.100 (4)
Fe(1)–C(9)	2.034 (4)	S(1)–C(10)	1.724 (4)
S(2)–C(20)	1.718 (3)	S(3)–C(30)	1.712 (4)
O(1)–C(1)	1.140 (5)	O(2)–C(2)	1.147 (5)
O(3)–C(3)	1.142 (4)	N(11)–C(10)	1.321 (5)
N(12)–C(10)	1.326 (5)	N(21)–C(20)	1.325 (4)
N(22)–C(20)	1.331 (4)	N(31)–C(30)	1.325 (5)
N(32)–C(30)	1.330 (5)	C(4)–C(5)	1.409 (5)
C(4)–C(9)	1.398 (5)	C(5)–C(6)	1.507 (6)
C(6)–C(7)	1.540 (6)	C(7)–C(8)	1.501 (5)
C(8)–C(9)	1.423 (5)		
C(1)–Fe(1)–C(2)	102.4 (2)	C(1)–Fe(1)–C(3)	100.4 (2)
C(1)–Fe(1)–C(4)	131.8 (2)	C(1)–Fe(1)–C(5)	93.2 (2)
C(1)–Fe(1)–C(8)	92.3 (2)	C(1)–Fe(1)–C(9)	131.3 (2)
C(2)–Fe(1)–C(3)	91.4 (2)	C(2)–Fe(1)–C(4)	94.0 (2)
C(2)–Fe(1)–C(5)	95.3 (2)	C(2)–Fe(1)–C(8)	163.6 (2)
C(2)–Fe(1)–C(9)	123.7 (2)	C(3)–Fe(1)–C(4)	124.5 (2)
C(3)–Fe(1)–C(5)	163.3 (2)	C(3)–Fe(1)–C(8)	93.1 (2)
C(3)–Fe(1)–C(9)	93.8 (2)	C(4)–Fe(1)–C(5)	39.8 (2)
C(4)–Fe(1)–C(8)	70.5 (2)	C(4)–Fe(1)–C(9)	40.2 (2)
C(5)–Fe(1)–C(8)	76.5 (2)	C(5)–Fe(1)–C(9)	69.8 (2)
C(8)–Fe(1)–C(9)	40.2 (2)	Fe(1)–C(1)–O(1)	177.3 (4)
Fe(1)–C(2)–O(2)	178.1 (4)	Fe(1)–C(3)–O(3)	178.8 (4)
Fe(1)–C(4)–C(5)	72.9 (2)	Fe(1)–C(4)–C(9)	70.0 (2)
Fe(1)–C(5)–C(4)	67.3 (2)	Fe(1)–C(5)–C(6)	110.5 (3)
Fe(1)–C(8)–C(7)	109.2 (3)	Fe(1)–C(8)–C(9)	67.4 (2)
Fe(1)–C(9)–C(4)	69.7 (2)	Fe(1)–C(9)–C(8)	72.4 (2)
S(1)–C(10)–N(11)	120.5 (3)	S(1)–C(10)–N(12)	120.3 (3)
S(2)–C(20)–N(21)	120.6 (3)	S(2)–C(20)–N(22)	120.7 (3)
S(3)–C(30)–N(31)	120.7 (3)	S(3)–C(30)–N(32)	120.6 (3)
N(11)–C(10)–N(12)	119.2 (3)	N(21)–C(20)–N(22)	118.7 (3)
N(31)–C(30)–N(32)	118.6 (4)	C(5)–C(4)–C(9)	115.0 (3)
C(4)–C(5)–C(6)	119.3 (3)	C(5)–C(6)–C(7)	110.8 (3)
C(6)–C(7)–C(8)	110.4 (3)	C(7)–C(8)–C(9)	121.0 (4)
C(4)–C(9)–C(8)	115.3 (3)		

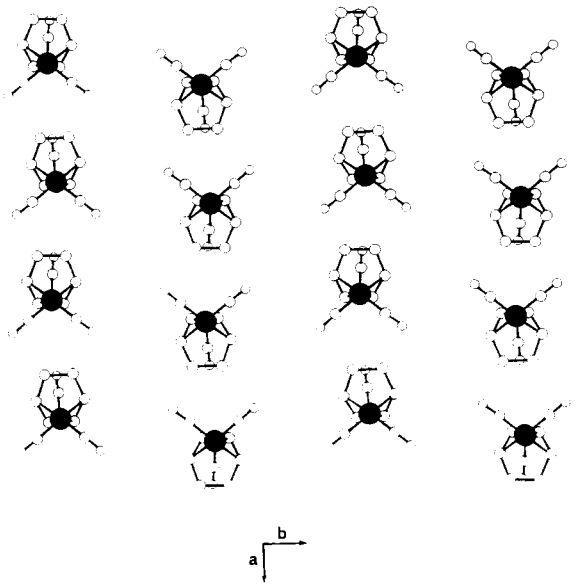

Figure 7. Arrangement of (η^4-1,3-cyclohexadiene)$Fe(CO)_3$ in **2**. Thioureas form channels along the *a* axis.

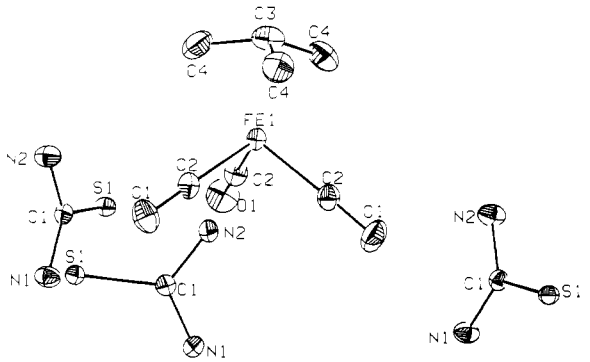

Figure 8. ORTEP of thiourea·(η^4-trimethylenemethane)$Fe(CO)_3$ (**3**).

Table V. Selected Interatomic Distances (angstroms) and Intramolecular Angles (degrees) for 3

Fe(1)–C(2)	1.784 (3)	Fe(1)–C(3)	1.926 (7)
Fe(1)–C(4)	2.105 (4)	S(1)–C(1)	1.718 (2)
O(1)–C(2)	1.138 (4)	N(1)–C(1)	1.317 (4)
N(2)–C(1)	1.323 (4)	N(1)–H(1)	0.896 (37)
N(1)–H(1′)	0.685 (46)	N(2)–H(2)	0.740 (35)
N(2)–H(2′)	0.949 (36)	C(3)–C(4)	1.427 (5)
C(4)–H(4)	0.952 (47)	C(4)–H(4′)	1.070 (54)
C(2)–Fe(1)–C(2)a	97.3 (1)	C(2)–Fe(1)–C(3)	119.9 (1)
C(2)–Fe(1)–C(4)	94.6 (2)	C(2)–Fe(1)–C(4)a	95.7 (2)
C(2)–Fe(1)–C(4)b	161.1 (2)	C(3)–Fe(1)–C(4)	41.2 (1)
C(4)–Fe(1)–C(4)a	69.5 (2)	Fe(1)–C(2)–O(1)	178.8 (4)
Fe(1)–C(3)–C(4)	76.2 (3)	Fe(1)–C(4)–C(3)	62.7 (3)
Fe(1)–C(4)–H(4)	113 (3)	S(1)–C(1)–N(1)	120.5 (2)
S(1)–C(1)–N(2)	120.4 (2)	N(1)–C(1)–N(2)	119.1 (3)
C(4)–C(3)–C(4)a	114.5 (2)		

ganometallic units is canted with respect to the next layer by some 60°. Each Fe molecule is related to its nearest neighbor by a glide plane or 2-fold screw axis. There is not a single polar direction common to all (η^4-1,3-cyclohexadiene)$Fe(CO)_3$ but two that average to an overall resultant polar axis pointing perpendicular to the channels along the *c* axis (Figures 6 and 7).

The structure of (thiourea)$_3$·(η^4-trimethylenemethane)-$Fe(CO)_3$ (**3**) was determined (Tables I and V). The structure of this inclusion complex containing a d^6 metal system is isomorphous with **1** (Figures 8 and 9). The guest molecules stack along the axes of the channels (*c* axis) with

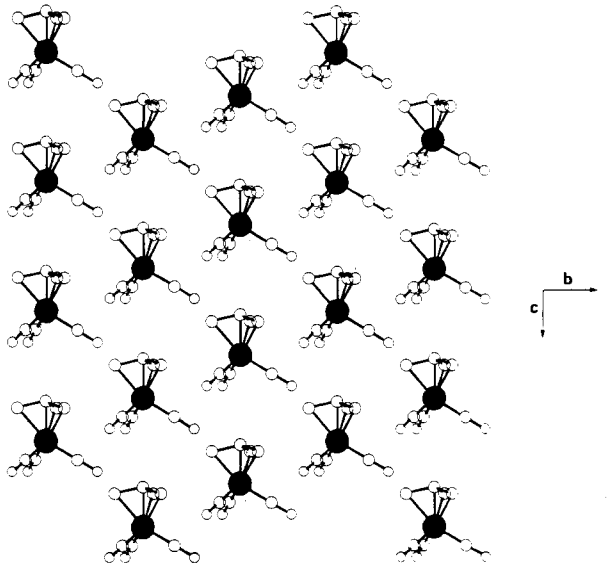

Figure 9. Arrangement of (η^4-trimethylenemethane)Fe(CO)$_3$ in **3**.

Table VI. Selected Interatomic Distances (angstroms) and Intramolecular Angles (degrees) for 4

Mn(1)–C(1)	1.756 (10)	Mn(1)–C(2)	2.308 (11)
Mn(1)–C(3)	2.202 (9)	S(1)–C(4)	1.721 (6)
O(1)–C(1)	1.161 (11)		
N(1)–C(4)	1.350 (9)	N(2)–C(4)	1.282 (10)
C(2)–C(3)b	1.377 (13)	C(2)–C(3)	1.427 (15)
Mn(1)–C(1)–O(1)	177 (1)	S(1)–C(4)–N(1)	119.1 (5)
S(1)–C(4)–N(2)	121.1 (5)	N(1)–C(4)–N(2)	119.8 (5)
C(3)–C(2)–C(3)b	119 (1)	C(2)–C(3)–C(2)a	119 (1)

a separation distance of 3.18 Å between the plane of the carbonyl oxygen atoms and adjacent methylene groups. The host channel thiourea hydrogen bonding is similar to those found in **1** with S–N distances ranging from 3.4 to 3.5 Å. The trimethylenemethane ligand is puckered with the central atom 0.34 Å out of the plane of the methylene atoms, resulting in Fe–C distances of 1.93 and 2.11 Å. The twist angle between the carbonyl and the "spoke" of the trimethylenemethane is 58.9°. The angle between carbonyl groups of adjacent molecules is 16.7° (this is the staggering angle between guests).

We can speculate as to why (η^4-1,3-cyclohexadiene)Fe(CO)$_3$ prefers to stack sideways as opposed to the stacking found for (η^4-trimethylenemethane)Fe(CO)$_3$. The iron in (η^4-1,3-cyclohexadiene)Fe(CO)$_3$ is formally a d^8 metal center while in (η^4-trimethylenemethane)Fe(CO)$_3$ is a d^6. One, therefore, expects more back-donation to the π^* orbital of carbon monoxide in the Fe(d^8) system than in the Fe(d^6) system. The oxygen of the carbonyl ligands in the Fe(d^8) system would be expected to be better Lewis bases and be more prone to hydrogen bonding with the thioureas. By stacking sideways in the channel of **2**, (η^4-1,3-cyclohexadiene)Fe(CO)$_3$ can hydrogen bond with the thiourea units and gain extra stabilization over the collinear stacking experienced by (η^4-trimethylenemethane)Fe(CO)$_3$ in **3**. The carbonyl stretching vibrations for **2** are at lower frequencies than for **3** by about 20 cm^{-1}; this is consistent with back-donation being more important for (η^4-1,3-cyclohexadiene)Fe(CO)$_3$ than for (η^4-trimethylenemethane)-Fe(CO)$_3$.

The structures of the complex of (thiourea)$_3$·(η^5-cyclohexadienyl)Mn(CO)$_3$ (**4**, Figure 10) was determined (Tables I and VI) and found to be isomorphous with the (η^6-benzene)Cr(CO)$_3$ case (**1**). The staggering of adjacent Mn molecules along the channel is 35.1°, while the S–N intermolecular distances range from 3.46 to 3.54 Å. The internal diameter of the channels is 9.48 Å. The slight increase in cell volume for **4** over **1** may result from the larger organic ligand size of **4**.

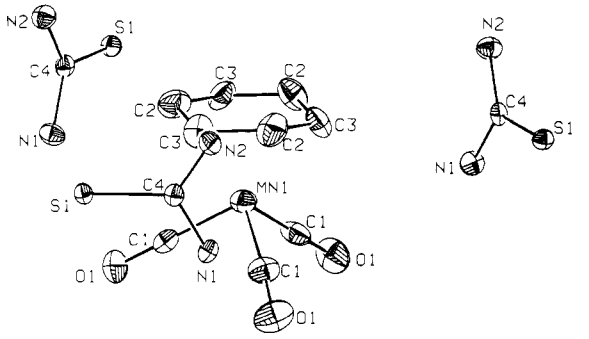

Figure 10. ORTEP of thiourea·(η^5-cyclohexadienyl)Mn(CO)$_3$ (**4**).

The N–O intermolecular distances for **1** are 3.12, 3.26, and 3.45 Å; for **4**, they are 3.23, 3.28, and 3.31 Å. The N–O distances for **3** are 3.01, 3.24, and 3.40 Å. The shortest such distances are observed for **2**, where the closest N–O distances are 2.97, 3.05, 3.06, 3.10, and 3.19 Å. Also, as observed in Figure 6, the oxygens of (η^4-1,3-cyclohexadiene)Fe(CO)$_3$ are pointed in the voids where the hydrogens of thioureas are located. Once again, this is evidence for hydrogen bonding being more important in **2** than in either **1**, **3**, or **4**.

As can be seen from the four determined crystal structures, thiourea inclusion complexation of organometallics is an effective method of dipolar alignment of the guest to give materials suitable for SHG. Irradiation of the unincluded guests listed in Table III did not give any detectable second harmonic signals while (η^4-butadiene)-Fe(CO)$_3$, (η^4-1,3-cyclohexadiene)Fe(CO)$_3$, and (η^4-trimethylenemethane)Fe(CO)$_3$ are liquids at room temperature and therefore incapable of SHG. The ferrocene–thiourea compound does not generate any second harmonic signal. Ferrocene is a symmetrical molecule with no second-order hyperpolarizability. It is therefore incapable of SHG. However, the lack of SHG for ferrocene–thiourea also indicates that the thioureas are not oriented properly to produce a large bulk nonlinear susceptibility. In the ferrocene complex and in the four structures **1**–**4** determined here, the thioureas are not responsible for the SHG. In these structures, the thiourea channels are formed from helical H-bonded strands of thioureas. Each channel has helices of one-handedness, each with its own polar director running along the channel axis. Adjacent channels have counterpropagating helices, so the polar directors associated with the thiourea matrix does not contribute to bulk SHG in these complexes. All SHG is a property only of the guest.

These experiments clearly demonstrate the dramatic effect of inclusion complexation on the macroscopic nonlinear optical properties of these organometallics. These results also show that organometallics can possess nonlinear hyperpolarizabilities that can be useful in potential applications.

In certain cases, volatile guests can escape the channels. Light yellow crystals of the thiourea complexes of (η^4-butadiene)Fe(CO)$_3$ and (η^4-trimethylenemethane)Fe(CO)$_3$ will eventually become colorless if allowed to stand at room temperature for weeks. ^{1}H NMR spectra of the resultant white solids in deuterated methanol showed clean loss of guests.

(η^5-Cp)M(η^4-1,3-cyclohexadiene) (M = Co, Rh), (η^5-Cp)Rh(η^2-ethylene)$_2$, and (η^5-Cp)$_2$WH$_2$ can be included

Table VII. Inclusion Complexes with Tris-*o*-thymotide

guest	host:guest	SHG rel to urea
(*p*-cyanobenzoyl)Mn(CO)$_5$	ND[a]	0.2
(η^6-indan)Cr(CO)$_3$	1:1	0.1
(η^6-anisole)Cr(CO)$_3$	1:1	0.1
(η^6-tetralin)Cr(CO)$_3$	1:1	0.1
(η^6-(dimethylamino)benzene)Cr(CO)$_3$	1:1	0.13
[(η^6-benzene)Mn(CO)$_3$]BF$_4$	ND	0.1
W(CO)$_5$(pyridine)	2:1[b]	0.0
W(CO)$_5$(4-picoline)	1:1	0.0
W(CO)$_5$(4-aminopyridine)	2:1[b]	0.0
W(CO)$_5$(4-ethylpyridine)	1:1	0.0
(η^6-*cis*-stilbene)Cr(CO)$_3$	ND	0.0
(η^6-*trans*-stilbene)Cr(CO)$_3$	1:1	0.0

[a] ND = not determined. [b] There are also two molecules of MeOH.

with thiourea, but the resultant complexes were SHG inactive. The reasons for these not being SHG active are (1) these guests do not possess an appreciable second-order polarizabilities, β, and/or (2) these materials crystallize centrosymmetrically. (η^5-Cp)M(η^4-1,3-cyclohexadiene)·thiourea (M = Co, Rh) complexes are unusual also because they are 4:1 host-to-guest complexes and not the typical 3:1 host-to-guest complexes normally observed for organometallic/thiourea compounds prepared in this study. Unfortunately, single crystals suitable for X-ray structural studies of these complexes could not be grown.

In general, thiourea inclusion complexes of organometallics can be prepared by cooling a 50% saturated solution of thiourea containing the organometallic in methanol. Obviously, organometallics not soluble in methanol cannot be included with thiourea with use of this procedure. We have also found that new guests can be incorporated by taking a preformed thiourea channel complex and treating it with an ether solution of the new guest. For example, when 100 mg of isooctane·thiourea was allowed to sit in an ether solution containing 100 mg of (η^6-benzene)Cr(CO)$_3$ for 3 days, the resultant solid collected by filtration was determined by ^{1}H NMR in deuterated methanol to be 6.5 thiourea/(η^6-benzene)Cr(CO)$_3$ with no isooctane. X-ray powder diffraction data indicated this to be a mixture of thiourea and the inclusion complex 1 of thiourea/(η^6-benzene)Cr(CO)$_3$. This material gave an SHG powder efficiency of 2 × urea, nearly identical with material prepared by the direct cocrystallization of (η^6-benzene)Cr(CO)$_3$ and thiourea. Similar treatment of isooctane·thiourea with (η^5-Cp)$_2$MoH$_2$ yielded a material with 4.5 thiourea/(η^5-Cp)$_2$MoH$_2$ as determined by its ^{1}H NMR spectrum in deuterated methanol (SHG: not active). Once again, this is most likely a mixture of thiourea and the inclusion compound. This complex (thiourea·(η^5-Cp)$_2$MoH$_2$) cannot be prepared by the conventional methanol route because (η^5-Cp)$_2$MoH$_2$ crystallizes out of solution in preference to the inclusion complex. If isooctane·thiourea was allowed to sit in an ether solution, the resultant solid is thiourea, indicating that the isooctane guests can escape from the channels. Finally, thiourea·(η^6-benzene)Cr(CO)$_3$ can be prepared by guest exchange with thiourea·(η^4-1,3-cyclohexadiene)Fe(CO)$_3$ (^{1}H NMR spectrum in deuterated methanol indicates 4.6 thiourea/(η^6-benzene)Cr(CO)$_3$; SHG: 0.7 × urea). Similar exchanges of hydrocarbon guest from preformed thiourea channels have been observed;[33] however, these are the first examples of exchange with polar guests to yield materials suitable for second harmonic generation. The nature of this unusual crystal-to-crystal transformation is under study.

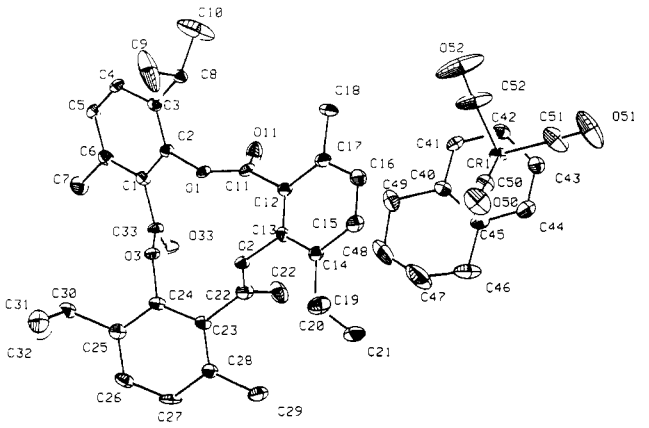

Figure 11. ORTEP of TOT·(η^6-tetralin)(Cr(CO)$_3$ (**5**).

Tris-*o*-Thymotide Inclusion Complexation of Organometallics. We have also studied inclusion of organometallics with TOT, which is known to form both cage-type[34] and channel-type clathrates.[26,34c] TOT inclusion complexes of organometallics prepared in this study are listed in Table VII along with the observed complex stoichiometry and results of SHG screening.

As was the case for thiourea complexes, the choice of guest for TOT is limited to those molecules whose shapes are compatible with TOT cavities. The voids (channels or cavities) formed by TOT are expected to be larger than those of thiourea[34] and to be somewhat flexible and expandable, since only van der Waals forces (rather than H-bonding forces as in thiourea) support complexation. We have included (substituted-benzene)chromium tricarbonyl complexes and (substituted-pyridine)tungsten pentacarbonyls because their shapes are similar to other guests that have been included in this host. Also, we would be able to compare these results with the thiourea system. In addition, tungsten pyridine complexes should exhibit some modest molecular second-order hyperpolarizability because they are known to possess charge-transfer states.[3b,11]

TOT inclusion complexation has resulted (Table VII) in the preparation of materials suitable for SHG. The guests themselves are SHG inactive, and TOT (from slow evaporation of methanol solution) is only very weakly active (<0.006 × urea).[34a,35] However, the success rate for TOT complexation-induced SHG is lower than we experienced for thiourea complexation. This point will be discussed later.

The concept of dipolar alignment using channel inclusion complexation is not restricted to organometallics. We have prepared the TOT inclusion complexes with several representative organic molecules that possess para-disposed donor and acceptor functionalities: *trans-p*-(di-

(33) *Inclusion Compounds*; Atwood, J. L., Davies, J. E. D., MacNicol, D. D., Eds.; Academic Press: New York, 1984; Vol 2, Chapter 2.

(34) (a) Brunie, S.; Navaza, A.; Tsoucaris, G.; Declercq, J. P.; Germain, G. *Acta Crystallogr., Sect. B* **1977**, *33*, 2645. (b) Williams, D. J.; Lawton, D. *Tetrahedron Lett.* **1975**, 111. (c) *Inclusion Compounds*; Atwood, J. L., Davies, J. E. D., MacNicol, D. D., Eds.; Academic Press: New York, 1984; Vol. 2, Chapter 6.

(35) The structure of TOT has been determined: Brunie, S.; Tsoucaris, G. *Cryst. Struct. Commun.* **1974**, *3*, 481.

(36) Crystals of 2TOT·*p*-(dimethylamino)cinnamaldehyde with $Z = 4$, space group $P\bar{1}$ with $a = 13.199$ (2), $b = 23.473$ (4), $c = 11.5402$ (2) Å, $\alpha = 100.91$ (1), $\beta = 94.66$ (1), $\gamma = 81.63$ (1)°; from ref 25, $T = -100$ °C, final R for the isotropic refinement is 13.1%. The two independent cinnamaldehyde groups are disordered on inversion centers, and there were not enough data to attempt an ordered acentric refinement. However, the SHG activity dictates an acentric arrangement and suggest the correct structure as $P1$. Additional information on this disordered structure is supplied in the supplementary material.

Table VIII. Crystal Data and Summary of Intensity Data Collection and Structure Refinement for TOT Inclusion Complexes 5–9

	5	6	7	8	9
mol wt	796.88	1524.38	1539.39	945.67	959.70
space group	$Pca2_1$	$I2/a$	$I2/a$	$P2_1/c$	$P2_1/c$
cell consts					
a, Å	14.531 (3)	22.912 (4)	22.966 (13)	12.848 (5)	12.803 (2)
b, Å	20.356 (2)	13.714 (7)	13.916 (8)	23.912 (9)	24.201 (5)
c, Å	13.763 (2)	23.362 (7)	23.258 (13)	14.263 (5)	14.314 (4)
α, deg	90.0	90.0	90.0	90.0	90.0
β, deg	90.0	95.22 (2)	95.36 (4)	102.62 (3)	103.01 (2)
γ, deg	90.0	90.0	90.0	90.0	90.0
cell vol, Å^3	407.0	7310.3	7400.7	4276.0	4321.3
molecules/unit cell	4	4	4	4	4
D(calcd), g cm^{-3}	1.300	1.369	1.353	1.469	1.475
temp, °C	−100	−70	−100	−100	−70
μ(Mo)	3.26	16.80	16.59	28.15	27.86
2θ range, deg	4.0–52.0	2.4–54.0	4.8–54.0	4.2–53.0	1.7–55.0
total unique data	4502	8556	8654	9487	10581
unique data with $I \geq 3\sigma(I)$	2143	3225	5840	6085	5727
no. of parameters varied	504	447	466	514	523
R	0.048	0.052	0.035	0.026	0.037
R_w	0.045	0.043	0.031	0.028	0.036

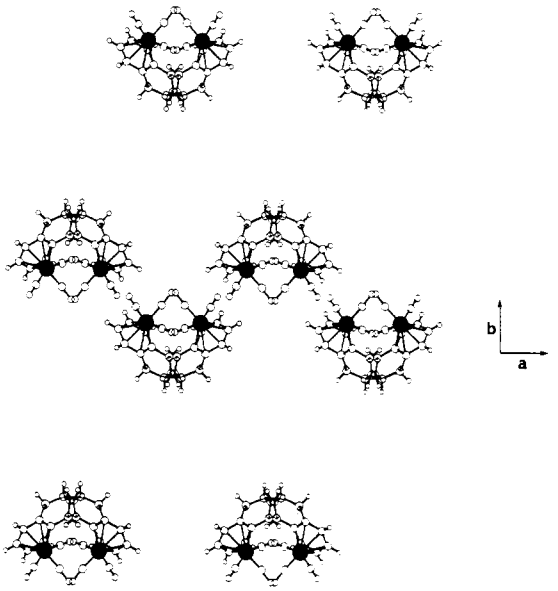

Figure 12. View down the channels of **5**. TOT deleted for clarity.

methylamino)cinnamaldehyde (SHG efficiency: 0.06–1.0 × urea) and *p*-(dimethylamino)benzonitrile (SHG: 0.3 × urea) as guests. Both of these complexes are 2:1 host-to-guest inclusion compounds.[36] Once again, the unincluded guests are not capable of generating second harmonic radiation presumably because they crystallize in centrosymmetric space groups.

The structure of TOT·(η^6-tetralin)Cr(CO)$_3$ (**5**) was determined (Figure 11). Crystal data and selected bond and angle information are listed in Tables VIII and IX. This is again a channel inclusion complex in which the channels are generated by the packing of the TOT host. The diameter of the channels is considerably larger (~18 vs ~9 Å) than those of the thiourea examples, and two (η^6-tetralin)Cr(CO)$_3$ can fit into these channels (Figure 12, view down the channels; TOT deleted for clarity). An adjacent channel is related by a glide plane operation with the closest Cr–Cr distance between channels of 8.199 Å. The closest Cr–Cr distance within two columns related by translation is 18.081 Å. There is not a single polar direction common to all (η^6-tetralin)Cr(CO)$_3$, but there are several that average to an overall resultant polar axis pointing parallel to the channels along the c axis. Viewing the structure along the channel direction (Figure 13, looking at one column along the c axis), we see that the (η^6-tetralin)Cr(CO)$_3$ molecules are staggered and slightly tilted toward one another (they are related by a glide plane

Table IX. Selected Interatomic Distances (angstroms) and Intramolecular Angles (degrees) for 5

Cr(1)–C(40)	2.248 (7)	Cr(1)–C(41)	2.185 (8)
Cr(1)–C(42)	2.215 (8)	Cr(1)–C(43)	2.190 (9)
Cr(1)–C(44)	2.219 (8)	Cr(1)–C(45)	2.255 (7)
Cr(1)–C(50)	1.802 (10)	Cr(1)–C(51)	1.837 (12)
Cr(1)–C(52)	1.816 (12)	O(1)–C(2)	1.406 (8)
O(50)–C(50)	1.151 (10)	O(51)–C(51)	1.134 (12)
O(52)–C(52)	1.141 (11)	C(1)–C(2)	1.399 (10)
C(40)–C(41)	1.403 (10)	C(40)–C(45)	1.426 (11)
C(40)–C(49)	1.536 (12)	C(41)–C(42)	1.401 (12)
C(42)–C(43)	1.384 (11)	C(43)–C(44)	1.384 (12)
C(44)–C(45)	1.391 (11)	C(45)–C(46)	1.528 (12)
C(46)–C(47)	1.459 (17)	C(47)–C(48)	1.419 (22)
C(48)–C(49)	1.478 (15)		
C(31)–C(30)–C(32)	111.3 (9)	C(41)–C(40)–C(45)	118.0 (8)
C(41)–C(40)–C(49)	120.5 (8)	C(45)–C(40)–C(49)	121.5 (7)
C(40)–C(41)–C(42)	122.5 (8)	C(41)–C(42)–C(43)	117.7 (8)
C(42)–C(43)–C(44)	121.6 (9)	C(43)–C(44)–C(45)	121.1 (9)
C(40)–C(45)–C(44)	119.1 (8)	C(40)–C(45)–C(46)	118.9 (9)
C(44)–C(45)–C(46)	122 (1)	C(45)–C(46)–C(47)	115 (1)
C(46)–C(47)–C(48)	117 (1)	C(47)–C(48)–C(49)	115 (1)
C(40)–C(49)–C(48)	112 (1)		

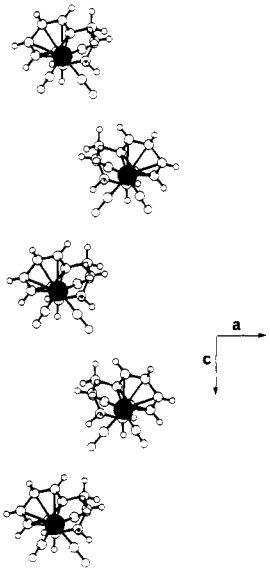

Figure 13. View along a channel of **5**. TOT deleted for clarity.

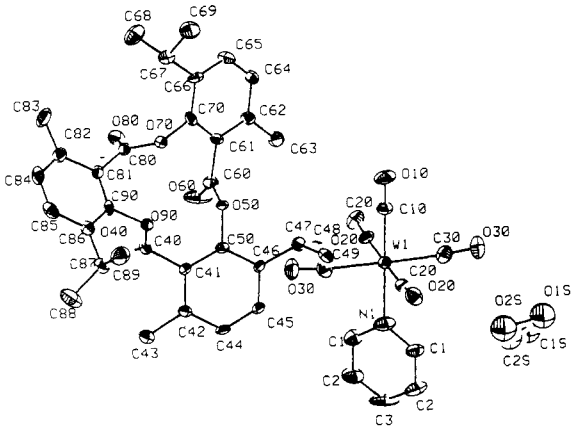

Figure 14. ORTEP of TOT·W(CO)$_5$(pyridine)·MeOH (6).

operation); Cr–Cr distance between molecules within a channel is 7.945 Å. The net effect is a zigzag head-to-tail dipolar alignment of the guests within the channels.

As noted in Table VII, the SHG powder efficiencies of these TOT complexes are relatively low (0.1–0.2 × urea). One possible reason for this is because the TOT host molecules are not oriented favorably to contribute to $\chi^{(2)}$ (also, TOT may not possess an appreciable molecular polarizability). Consequently, a large volume fraction of the crystal consists of an inactive component, unable to contribute to the nonlinearity and producing materials of low SHG efficiencies. We are presently attempting to design new hosts with high molecular polarizabilities and are trying to prepare materials where both the host and guest's molecular dipoles are oriented favorably to contribute to the noncritical phase-matched macroscopic nonlinear coefficient.

Within a pseudo-one-dimensional channel, the molecules would prefer to align head-to-tail to optimize electrostatic attraction if the diameter of the channels was not large enough to accommodate a head-to-tail antiparallel pair. A zigzag head-to-tail dipolar alignment of the guests within a channel as seen in the TOT·(η^6-tetralin)Cr(CO)$_3$ structure would result. If the diameter of the channels was just large enough to accommodate the guest, the optimum case of dipolar alignment would result as seen in the structure of

Table X. Selected Interatomic Distances (angstroms) and Intramolecular Angles (degrees) for 6

W(1)–N(1)	2.246 (13)	W(1)–C(10)	1.987 (15)
W(1)–C(20)	1.992 (8)	W(1)–C(30)	2.043 (10)
O(10)–C(10)	1.124 (15)	O(20)–C(20)	1.172 (8)
O(30)–C(30)	1.133 (9)	O(40)–C(40)	1.191 (9)
O(50)–C(50)	1.427 (8)	O(50)–C(60)	1.330 (10)
O(60)–C(60)	1.191 (10)	O(70)–C(70)	1.411 (8)
O(70)–C(80)	1.365 (9)	O(80)–C(80)	1.156 (9)
O(90)–C(40)	1.351 (9)	O(90)–C(90)	1.426 (9)
N(1)–C(1)	1.347 (11)	C(1)–C(2)	1.392 (13)
C(2)–C(3)	1.332 (13)	C(40)–C(41)	1.499 (10)
N(1)–W(1)–C(10)	180 (4)	N(1)–W(1)–C(20)	91.2 (3)
N(1)–W(1)–C(30)	90.8 (4)	C(10)–W(1)–C(20)	88.8 (3)
C(10)–W(1)–C(30)	89.2 (4)	C(20)–W(1)–C(20)a	177.6 (6)
C(20)–W(1)–C(30)a	89.1 (3)	C(20)–W(1)–C(30)	90.8 (3)
C(30)–W(1)–C(30)a	178.3 (8)	C(50)–O(50)–C(60)	116.9 (6)
W(1)–N(1)–C(1)	122.8 (7)	C(1)–N(1)–C(1)a	114 (1)
W(1)–C(10)–O(10)	180 (4)	W(1)–C(20)–O(20)	175 (1)
W(1)–C(30)–O(30)	175 (1)	O(40)–C(40)–O(90)	123.6 (8)
N(1)–C(1)–C(2)	124 (1)	C(1)–C(2)–C(3)	119 (1)
C(2)–C(3)–C(2)a	120 (2)	C(40)–C(41)–C(42)	118.9 (7)
C(40)–C(41)–C(50)	121.8 (7)	C(42)–C(41)–C(50)	119.3 (7)

(thiourea)$_3$·(η^6-benzene)Cr(CO)$_3$. However, if the channels were large enough to accommodate a head-to-tail antiparallel pair, a centrosymmetric structure would result. An example of this is the (TOT)$_2$·(W(CO)$_5$(pyridine))·(MeOH)$_2$ (6) inclusion complex. It is not SHG active. W(CO)$_5$(pyridine) is expected to possess a second-order polarizability because it is believed to have a metal-to-ligand charge-transfer state.[25] In fact, several metal pyridine and bipyridine complexes have been found to be capable of SHG.[3b] The crystal data and selected bond and angle data for this TOT inclusion complex are shown in Tables VIII and X. The molecular structure is shown in Figure 14. In this case, each W(CO)$_5$(pyridine) is related to its nearest neighbor by a 2-fold rotation. The closest W–W distance is 11.53 Å (Figure 15). The plane of the pyridine lies roughly normal to the stacking axis. The residual peaks have been located after the tungsten and TOT moieties have been found and are assumed to be due to the solvent of crystallization, methanol. Close contacts between this methanol and oxygens of TOT and carbonyl oxygens of W(CO)$_5$(pyridine) occur, indicative of hydrogen bonding. However, severe disorder of the methanol does not allow

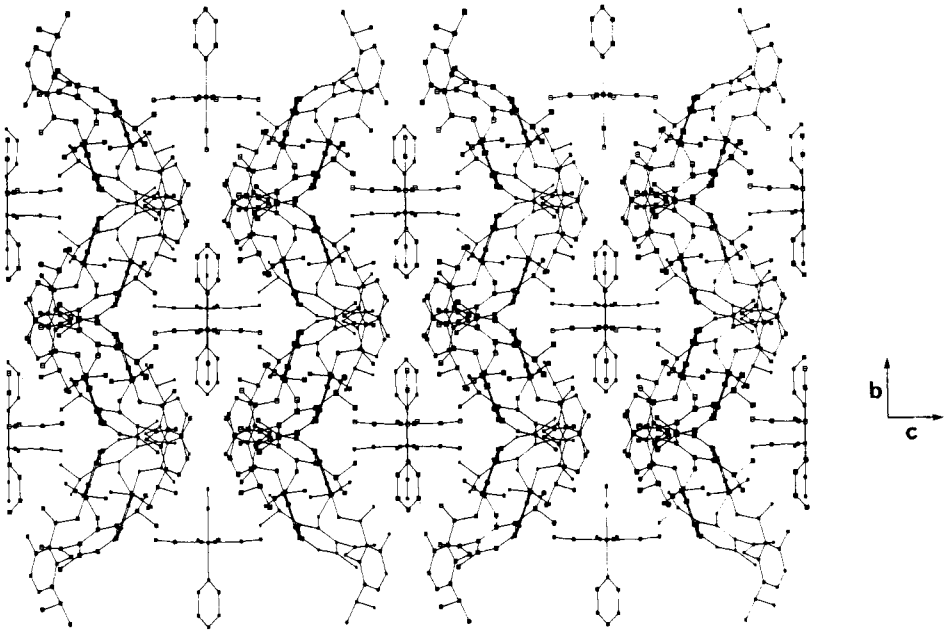

Figure 15. View down the channels of 6. Two W(CO)$_5$(pyridine) are shown in each channel for clarity. MeOH deleted for clarity.

Table XI. Selected Interatomic Distances (angstroms) and Intramolecular Angles (degrees) for 8

W(1)-N(1)	2.282 (3)	W(1)-C(10)	1.991 (4)
W(1)-C(11)	2.041 (4)	W(1)-C(12)	2.043 (4)
W(1)-C(13)	2.034 (5)	W(1)-C(14)	2.070 (5)
O(10)-C(10)	1.160 (5)	O(11)-C(11)	1.147 (5)
O(12)-C(12)	1.152 (5)	O(13)-C(13)	1.154 (5)
O(14)-C(14)	1.137 (5)	N(1)-C(1)	1.364 (5)
N(1)-C(5)	1.353 (5)	C(1)-C(2)	1.374 (6)
C(2)-C(3)	1.390 (5)	C(3)-C(4)	1.398 (6)
C(3)-C(6)	1.510 (5)	C(4)-C(5)	1.383 (6)
N(1)-W(1)-C(10)	179.4 (5)	N(1)-W(1)-C(11)	91.9 (1)
N(1)-W(1)-C(12)	94.1 (1)	N(1)-W(1)-C(13)	89.1 (2)
N(1)-W(1)-C(14)	90.9 (1)	C(10)-W(1)-C(11)	87.5 (2)
C(10)-W(1)-C(12)	86.5 (2)	C(10)-W(1)-C(13)	91.1 (2)
C(10)-W(1)-C(14)	88.9 (2)	C(11)-W(1)-C(12)	174.0 (2)
C(11)-W(1)-C(13)	88.9 (2)	C(11)-W(1)-C(14)	91.8 (2)
C(12)-W(1)-C(13)	90.5 (2)	C(12)-W(1)-C(14)	88.9 (2)
C(13)-W(1)-C(14)	179.4 (3)	W(1)-N(1)-C(1)	121.3 (3)
W(1)-N(1)-C(5)	123.1 (3)	C(1)-N(1)-C(5)	115.5 (3)
W(1)-C(10)-O(10)	179.7 (7)	W(1)-C(11)-O(11)	176.3 (4)
W(1)-C(12)-O(12)	175.2 (4)	W(1)-C(14)-O(14)	177.3 (5)
N(1)-C(1)-C(2)	123.3 (4)	C(3)-C(4)-C(5)	120.2 (4)
N(1)-C(5)-C(4)	123.9 (4)	C(1)-C(2)-C(3)	121.1 (4)
C(2)-C(3)-C(4)	115.9 (4)	C(2)-C(3)-C(6)	122.4 (4)
C(4)-C(3)-C(6)	121.7 (4)		

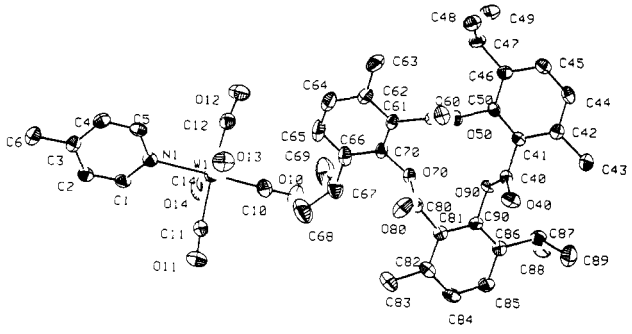

Figure 16. ORTEP of TOT·$W(CO)_5$(4-picoline) (8).

much confidence in any definitive assignment of discrete hydrogen-bonding structures. The structure can best be described as sheets of TOT molecules with the organometallic and solvent molecules lying in pockets between the sheets.

We attempted to "flip" the organometallic and induce head-to-tail dipolar alignment by making the molecule longer in the hope that a head-to-tail antiparallel pair would not be able to fit into the channel. Unfortunately, the TOT channels are much more flexible than those with thiourea since there is no hydrogen bonding operating in this case. The structure of the TOT inclusion complex of $W(CO)_5$(4-aminopyridine) (7) was found to be isomorphous with that of TOT·$W(CO)_5$(pyridine) (Table VIII). The unit cell volume increases by about 90 Å^3 primarily via a larger b axis, as expected since the molecule lies on the 2-fold axis along this direction. The W–W distance in this structure is 11.58 Å.

The TOT inclusion complexes with $W(CO)_5$(4-picoline) (8) and $W(CO)_5$(4-ethylpyridine) (9) have been prepared. In these two cases, another strong packing force comes into play that gives centrosymmetric structures. These two structures are isomorphous (Tables VIII and XI), and we will discuss only the $W(CO)_5$(4-picoline) (8) case in detail (Figure 16). This is once again a channel inclusion complex; a view of the organometallic packing is shown in Figure 17. The organometallics have indeed "flipped" as we have wanted. However, there are now π–π interactions between the pyridine rings of two organometallic guests, with planes of separation of 3.46 Å (3.56 Å in 9). This strong interaction leads to a centrosymmetric structure.

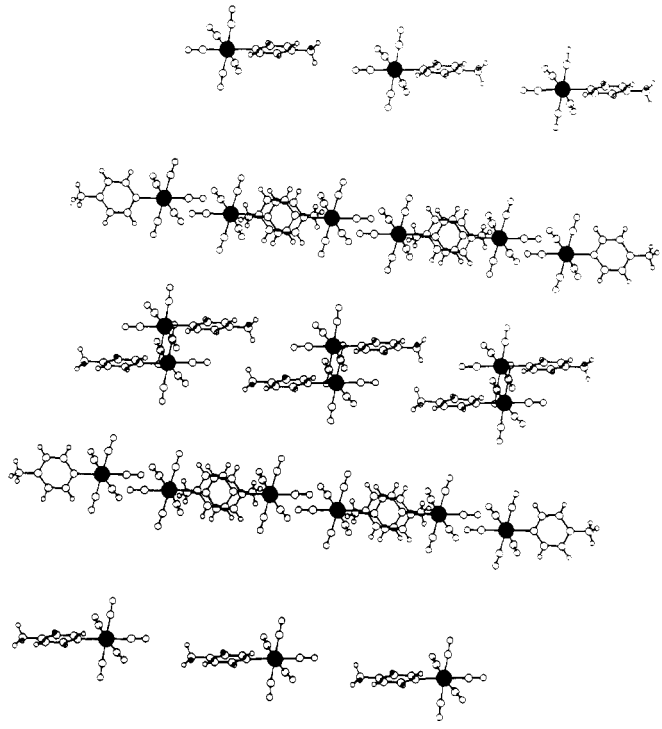

Figure 17. Looking along the channels of 8. View shows the π–π interaction of the pyridine rings.

There are now two different W–W distances of 10.08 and 6.71 Å (the W–W distances for 9 are 10.13 and 7.15 Å).[37]

Summary and Conclusions

Channel inclusion complexation has been found to enhance the probability of obtaining acentric crystal structures. In this pseudo-one-dimensional environment, the guest molecules prefer to have dipolar alignment along the channel direction. We have reported formation of 30 inclusion complexes between two hosts (thiourea and TOT) and various organometallic (28) and organic (2) guests. Of this total, 19 (63%) have proved to be SHG active. We have shown that five of the SHG-active compounds (all we examined in detail) crystallize in polar space groups. For thiourea complexation of organometallic guests, 11 of 16 (69%) inclusion complexes were active. For TOT–organometallic complexation, only 6 of 12 (50%) were active. We ascribe this difference to the strong tendency of dipoles to dimerize in an antiparallel (centrosymmetric) orientation. Tight control of channel dimensions are required to prevent this electrostatic interaction which leads to zero SHG. If channel dimensions can be controlled and maintained small relative to guest dimensions, then an alternate, head-to-tail dipolar orientation becomes electrostatically preferred. This leads to SHG-active materials.

The desired head-to-tail dipolar alignment arrangement may also not result if other strong packing forces are in play. We have seen two such examples in this study: (1) hydrogen bonding in the thiourea·(η^4-1,3-cyclohexadiene)$Fe(CO)_3$ complex and (2) π–π interaction of pyridine rings in TOT·$W(CO)_5$(4-picoline) and TOT·$W(CO)_5$(4-ethylpyridine) complexes.

In spite of these caveats, we note that our overall success rate for converting materials that are incapable of SHG into inclusion complexes that exhibit SHG is very high (63%) compared to nature's rate of formation of acentric

(37) Upon inclusion in the TOT host, a dramatic sharpening of the tungsten–pyridine emmission is observed; these results will be published separately by W. Tam and J. V Caspar.

structures (~24%).[38] We consider this to be an important achievement that points to new methodology, a paradigm of guest–host induced dipolar alignment, that can be used by chemists to engineer solid-state materials with specific properties.

Acknowledgment. The technical assistance of Barry Johnson, Louis Lardear, and Diane Peapus is acknowledged. Valuable discussions with Drs. David Thorn and Gerald Meredith are appreciated. Figures 2–4, 6, 7, 10, 12, 13, 15, and 17 were produced by using the CHEMGRAF suite of molecular modeling software, by E. Keith Davies (program MODEL, 1983, 1984) and the Chemical Crystallography Laboratory, University of Oxford (1982). These programs are used under licence.

Supplementary Material Available: Tables of positional and anisotropic thermal parameters as well as tables of bond distances and bond angles for **1–9** (63 pages). Ordering information is given on any current masthead page.

(38) Mighell, A. D.; Himes, V. L.; Rodgers, J. R. *Acta. Crystallogr., Sect. A* **1983**, *A39*, 737.

Syntheses, Structures, Selected Physical Properties, and Band Electronic Structures of the Bis(ethylenediseleno)tetrathiafulvalene Salts $(BEDSe\text{-}TTF)_2X$, $X^- = I_3^-$, AuI_2^-, and IBr_2^-

Hau H. Wang, Lawrence K. Montgomery, Urs Geiser, Leigh C. Porter, K. Douglas Carlson, John R. Ferraro, Jack M. Williams,* Carolyn S. Cariss, Rona L. Rubinstein, and Julia R. Whitworth

Chemistry and Materials Science Divisions, Argonne National Laboratory, Argonne, Illinois 60439

Michel Evain, Juan J. Novoa, and Myung-Hwan Whangbo*

Department of Chemistry, North Carolina State University, Raleigh, North Carolina 27650-8204

Received August 18, 1988

Three bis(ethylenediseleno)tetrathiafulvalene (BEDSe-TTF) based salts, $(BEDSe\text{-}TTF)_2X$ ($X^- = I_3^-$, AuI_2^-, and IBr_2^-), have been prepared by electrocrystallization and characterized by X-ray crystallography, electrical conductivity measurements, variable-temperature electron spin resonance studies, and FT-IR reflectance measurements. The triclinic (space group $P\bar{1}$) room-temperature lattice parameters for the three salts are as follows: β-$(BEDSe\text{-}TTF)_2I_3$: a = 6.781 (2) Å, b = 8.767 (3) Å, c = 16.023 (5) Å, α = 89.68 (2)°, β = 94.76 (2)°, γ = 110.66 (2)°, V = 887.9 (5) Å^3. $(BEDSe\text{-}TTF)_2AuI_2$: a = 7.614 (1) Å, b = 8.341 (2) Å, c = 15.538 (4) Å, α = 77.56 (2)°, β = 98.31 (2)°, γ = 112.71 (2)°, V = 886.9 (4) Å^3. β'-$(BEDSe\text{-}TTF)_2IBr_2$: a = 6.863 (2) Å, b = 10.065 (3) Å, c = 13.183 (3) Å, α = 87.94 (2)°, β = 100.49 (2)°, γ = 98.84 (2)°, V = 884.8 (4) Å^3. At room temperature, β-$(BEDSe\text{-}TTF)_2I_3$ is metallic and $(BEDSe\text{-}TTF)_2AuI_2$ and β'-$(BEDSe\text{-}TTF)_2IBr_2$ are semiconductors. Antiferromagnetic couplings were observed in both AuI_2^- and IBr_2^- salts at 20 and 12 K, respectively. Tight-binding band calculations were performed on the donor layers of the $(BEDSe\text{-}TTF)_2X$ salts in an attempt to understand the electrical properties. The relationships between the crystal structures, physical properties, and band electronic structures are discussed.

Introduction

The radical-cation salts of bis(ethylenedithio)tetrathiafulvalene (1, commonly abbreviated BEDT-TTF or,

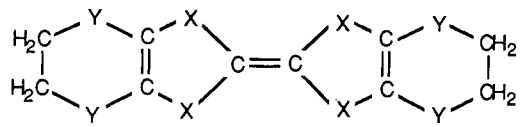

1, BEDT-TTF (ET), X = Y = S
2, BEDSe-TSeF, X = Y = Se
3, BEDSe-TTF, X = S, Y = Se

simply, ET) have been studied intensively,[1] since ambient-pressure bulk superconductivity ($T_c \sim 1.5$ K) was first discovered[2] and confirmed[3] in β-$(ET)_2I_3$ in 1984. κ-$(ET)_2Cu(NCS)_2$, the newest member of the ET family of superconductors, has an ambient-pressure superconducting transition temperature over 10 K.[4] In addition, more than half of the known ambient-pressure organic superconductors[5] are derived from ET, e.g., α_t-$(ET)_2I_3$ (T_c

(1) Williams, J. M.; Wang, H. H.; Emge, T. J.; Geiser, U.; Beno, M. A.; Leung, P. C. W.; Carlson, K. D.; Thorn, R. J.; Schultz, A. J. *Prog. Inorg. Chem.* **1987**, *35*, 51.

(2) Yagubskii, E. B.; Shchegolev, I. F.; Laukhin, V. N.; Kononovich, P. A.; Karatsovnik, M. W.; Zvarykina, A. V.; Buravov, L. I. *Pis'ma Zh. Eksp. Teor. Fiz.* **1984**, *39*, 12; *JETP Lett. (Engl. Transl.)* **1984**, *39*, 12.

(3) Williams, J. M.; Emge, T. J.; Wang, H. H.; Beno, M. A.; Copps, P. T.; Hall, L. N.; Carlson, K. D.; Crabtree, G. W. *Inorg. Chem.* **1984**, *23*, 2558.

(4) Urayama, H.; Yamochi, H.; Saito, G.; Nozawa, K.; Sugano, T.; Kinoshita, M.; Sato, S.; Oshima, K.; Kawamoto, A.; Tanaka, J. *Chem. Lett.* **1988**, 55.

(5) Other known ambient-pressure organic superconductors are derived from TMTSF,[6] DMET,[7] and MDT-TTF.[8]

0897-4756/89/2801-0140$01.50/0